Chapter 5. Photoemission Studies on Copper Porphyrazine Compounds

5.1 Valence Region

In order to investigate the fundamental aspects of the interactions between a central metal atom and the ligand, the compounds in the series were synthesized with Cu as center metal. The presence of copper in the molecule turns out to stabilize the larger complex in the series, which in fact enables the study of a wider range of linearly benzoannelated molecules: P0-Cu, P1-Cu, P2-Cu and P3-Cu. Even if the photoemission studies on such tert-butyl containing molecules are scarce, copper phthalocyanine (CuPc) is an intensively studied material both experimentally and theoretically, [RDR94, CLÅ2001, KSG2001], and this constitutes an important basis in the interpretation of the data.

Effect of Tert-butyl Substitution on the Photoemission Spectra

Similar to the case of metal-free molecules, the first step in the present photoemission studies was to investigate the effects of the tert-butyl substitution on the electronic structure of the compounds. For that purpose both CuPc and P1-Cu spectra were measured. The results are shown in Fig. 5.1-1 for 70.7 eV excitation energy. The spectra were obtained in normal emission. The angle of incidence was 83° and the polarization of the synchrotron light was perpendicular to the surface normal. The energy scale denotes the electron binding energies with respect to the vacuum level. To allow direct comparison of the spectra, they were normalized at the maximum of feature H, which appears to be a good choice considering the comparison between H_2Pc and P1-H_2 compounds. The spectra are vertically displaced with respect to each other (top CuPc and bottom P1-Cu compound), and additionally, in the lower panel the CuPc spectrum (dotted) is plotted on

59

the top of P1-Cu spectrum to emphasize the changes in the photoemission features resulting from tert-butyl substitution. To simplify the discussion, the bands have been denoted with capital letters. It should be noted that identical labels as compared to H_2Pc or P1-H_2 spectrum (in the Chapter 4) do not necessarily imply identical peak origin or energy. Only the bands A, B, D, G, H for the CuPc spectrum have about the same binding energies as in the H_2Pc photoemission spectrum. Significant differences exist in origin or binding energy between the bands C, E, F, F' in the CuPc spectrum and the equally denoted bands in the H_2Pc spectrum.
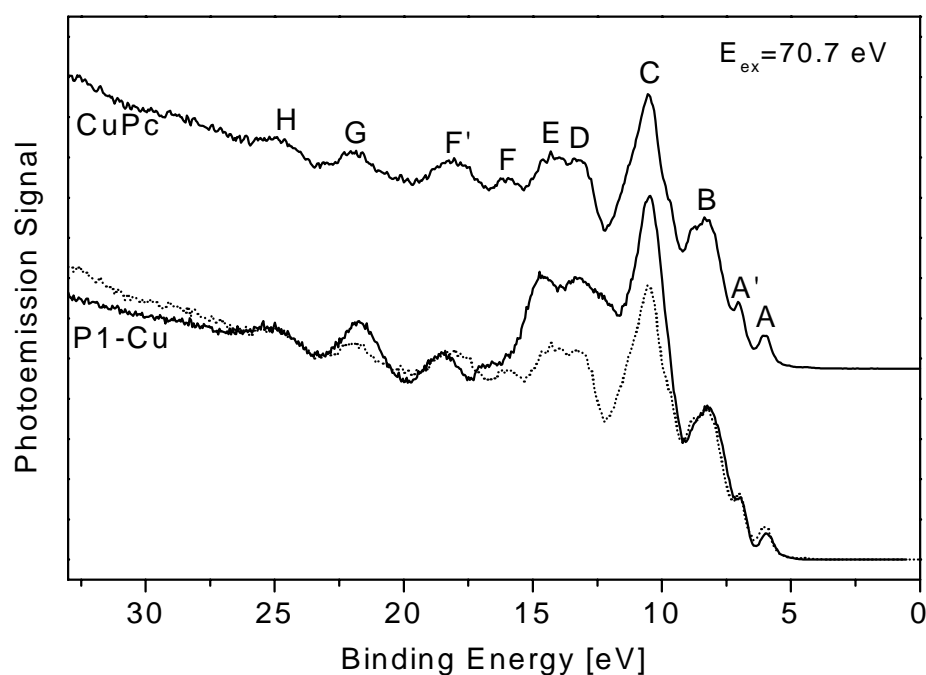

Fig. 5.1-1 Photoemission spectra from unsubstituted CuPc film (top) and P1-Cu film (bottom), both taken at 70.7 eV photon energy.

By comparing the photoemission spectra of CuPc and of P1-Cu (tert-butyl substituted CuPc), the changes introduced in the spectrum by the tert-butyl substitution can clearly be detected. Similar to the case of metal-free compounds, the tert-butyl influence is manifested predominantly as an intensity increase at the position of feature G and in the 9.5-16 eV binding energy range. Largely, the binding energies of most of the peaks are the same in CuPc and P1-Cu. Feature G is shifted by approximately 0.2 eV towards lower binding energies while peaks E and F' are shifted by ~0.3 and ~0.4 eV, respectively, towards larger binding energies. Due to the tert-butyl addition the band F is not resolved

anymore. The reason for the narrowing of band F' in P1-Cu compared to the CuPc is hard to infer.

Metal Features in the Spectra and Assignment of the Peaks

The P3-Cu film was prepared by the wet chemical method described in Chapter 3, whereas the other films were obtained by vacuum sublimation. To be sure that the wet chemical method does not introduce drastic changes in the photoemission spectra, we have prepared a P2-Cu film also by the wet chemical method. The photoemission spectrum of this film was measured and then it was compared with that of a P2-Cu film obtained by sublimation in UHV. The experimental data obtained with 75.8 eV photons are displayed in Fig. 5.1-2. The photoemission features turned out to be similar for the films prepared by the two methods. Based on this result it was concluded that also a P3-Cu film prepared by this method would be suitable for the photoemission measurements and its spectrum could be qualitatively compared with the spectra of P0-Cu, P1-Cu and P2-Cu.
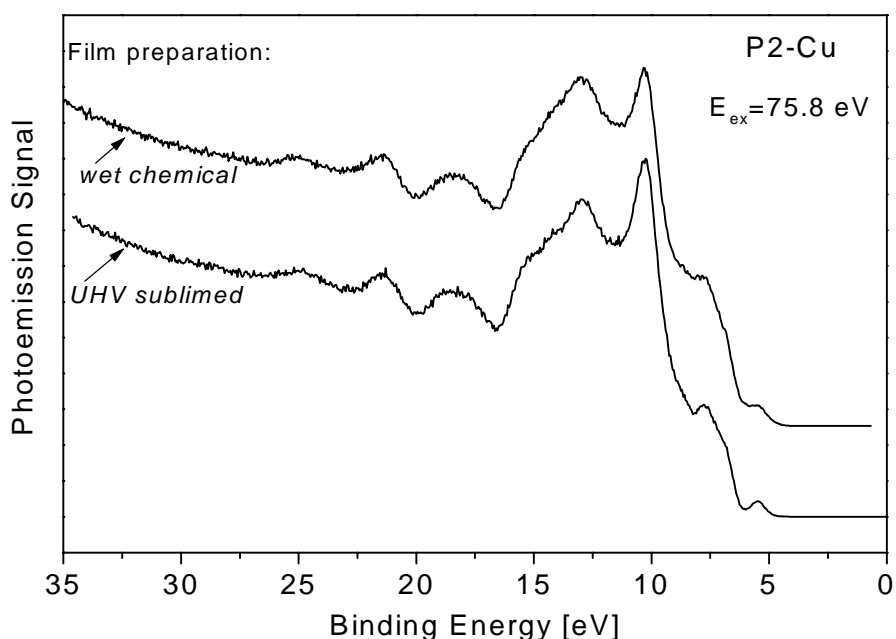

Fig. 5.1-2 Photoemission spectra from a P2-Cu film prepared by sublimation in UHV and from a P2-Cu film obtained by the wet chemical method described in Chapter 3.

In Fig. 5.1-3 are compared the photoemission spectra of CuPc and H_2Pc at 70.7 eV excitation energy. By this comparison the features arising from Cu can be distinguished. Due to the intrinsically different background, the normalization at a certain ligand peak did not lead to a good overlap of the two spectra.
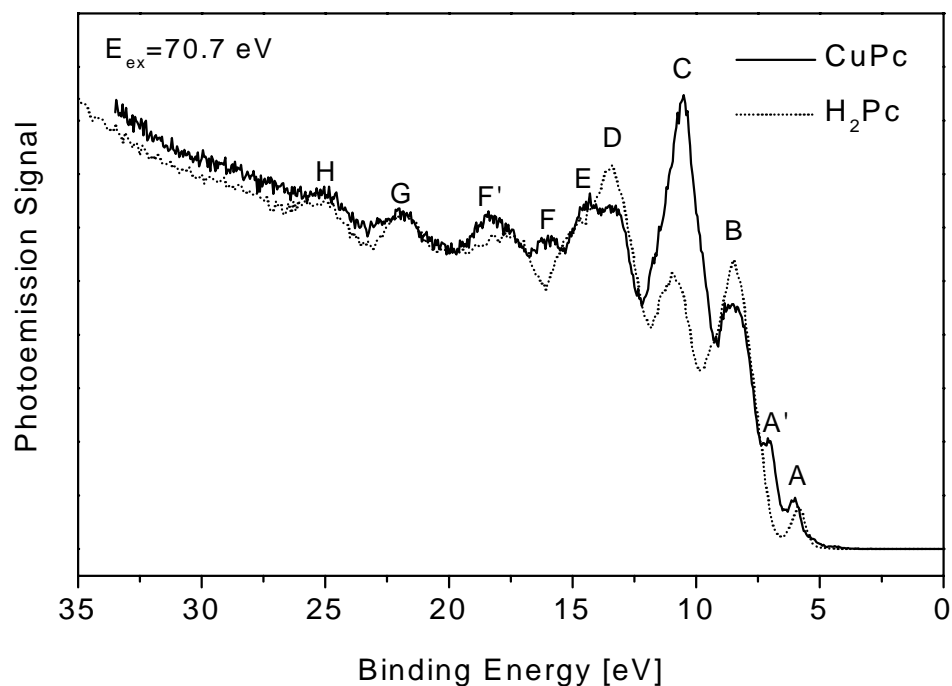
Fig. 5.1-3 Comparison of photoemission spectra of unsubstituted CuPc and H_2Pc.

Fig. 5.1-4 depicts the photoemission spectra of the P0-Cu, P1-Cu, P2-Cu, and P3-Cu together with the data for the corresponding metal-free compounds measured at 70.7 eV excitation energy. The films for the first three compounds in the series have been prepared by evaporation while that of the P3-Cu was produced by the wet chemical method. The P3-H_2 spectrum is missing, as this compound is unstable at film preparation. The binding energy scale in the case of P3-Cu was fixed by shifting the spectrum so that the binding energies of features G and H coincide with respect to the ones for P1-Cu and P2-Cu compounds. This is justified considering that G and H have important contributions from the benzene moieties.

From a comparison of the spectra in Fig. 5.1-4, at first glance it appears that the spectra of the Cu compounds can be regarded as the result of the mere addition of Cu contributions to the metal-free spectra. Similar considerations were also made for various transition-metal phthalocyanines in the gas phase [Ber79].
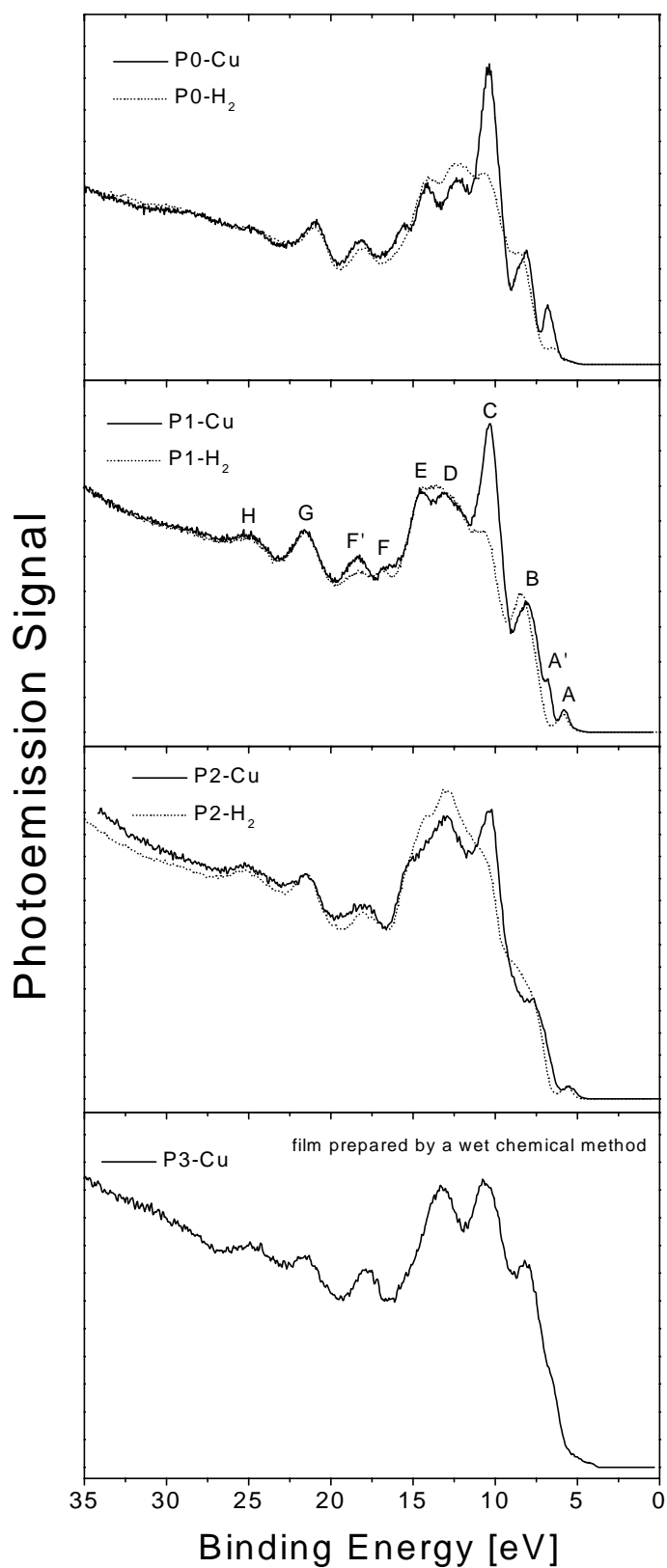
Fig. 5.1-4 Photoemission spectra from the Cu compounds in the series along with their metal-free counter parts. The data were taken for 70.7 eV excitation energy. The P3-H_2 spectrum is missing due to its instability at film preparation. The P0-Cu, P1-Cu and P2-Cu films were produced by sublimation, while that of P3-Cu is prepared by the wet chemical method.

Recent theoretical calculations showed that in the ground state the HOMO in CuPc is singly occupied having metal 3d-character. Under D_{4h} symmetry it is described as an antibonding Cu-N_p state having 44% Cu $d_{x^2-y^2}$ character and 56% Pc b_{1g} character [LiS2001] or 49% Cu $d_{x^2-y^2}$ character and 51% b_{1g} N_p-lone pair character (N_p denotes a pyrrol nitrogen) [RoB94]. In this light, the HOMO for CuPc can be sketched as shown in Fig. 5.1-5.
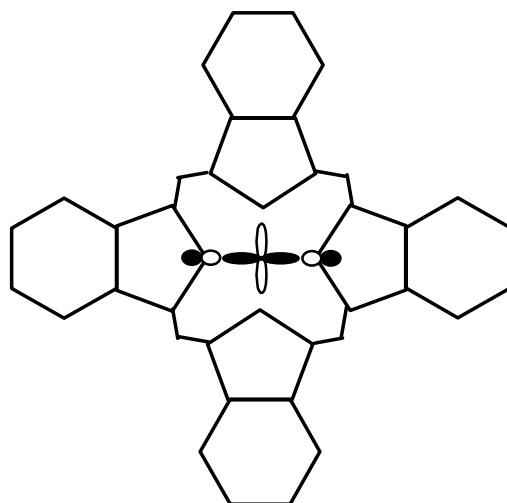

Fig. 5.1-5 Sketch of the HOMO for CuPc

HOMO-1 is a pure macrocycle a_{1u} orbital having in fact the same composition as the HOMO of metal-free phthalocyanine (spread over the carbon backbone). The HOMO-2 is a b_{2g} orbital which largely arises from the meso-bridging nitrogen [RoB94].

In CuPc the first ionization removes an electron from the phthalocyanine a_{1u} orbital although b_{1g} lies about 0.5 eV higher. It has been calculated that the ionization from b_{1g} requires 0.71 eV more than that from a_{1u} [LiS2001] (or 0.61 eV more in [RoB94]). The a_{1u} is determined to have an ionization energy of 6.51 eV [LiS2001], or 6 eV in [RoB94]. The next occupied orbitals are largely attributed to the ligand. The other copper d-like ionizations have energies that differ by (1.64-4.38) eV from the energy of b_{1g}.

In the case of copper tetraazaporphyrin (copper porphyrazine) the calculations evidenced also b_{1g} as the highest occupied level with important Cu $d_{x^2-y^2}$ electron contribution, determined as 52% in [BeE81] or 45% in [LFE91].

In accordance with the theory [LiS2001, RoB94, OrB92] and with previous experiments on CuPc [IKC80], and also taking into account the similarity between the molecules in the Cu series and CuPc, an assignment of the peaks in the spectra of the investigated Cu-porphyrazines can be done. It results that band A in Fig. 5.1-4 is derived

from the a_{1u} orbital (which has the same composition as the HOMO of metal-free compounds), while A' is derived from the HOMO of the copper molecules (b_{1g}). Bands A and A' are found roughly at 1 eV difference in energy in the spectrum for P1-Cu. It is assumed that peak B includes the contributions from benzene and meso-nitrogen atoms, similarly to metal-free compounds. At the position of band C, in addition to the benzene and nitrogen contributions, strong copper d-like emission is found [IKC80]. For CuPc, P0-Cu, P1-Cu and P2-Cu, the bands F and F' are composed of ligand contributions as well as Cu satellite signals. All the other peaks have the same origin as in case of the metal-free compounds (see Chapter 4).

Fig. 5.1-6 displays spectra of the P1-Cu compound obtained for three excitation energies. One can note that the intensity of peak C increases relative to the ligand features for increasing photon energy. The ratio between the cross sections of Cu3d and of carbon C2s or C2p orbitals increases with the photon energy in the energy range applied in the present experiments [Yeh93]. Therefore the behavior noted for band C is perfectly explained by its nature, namely that it contains the contributions from Cu3d direct emission. The variations seen in the intensity of the Cu satellites at the change of photon energy will be discussed in detail in a later section of this chapter.
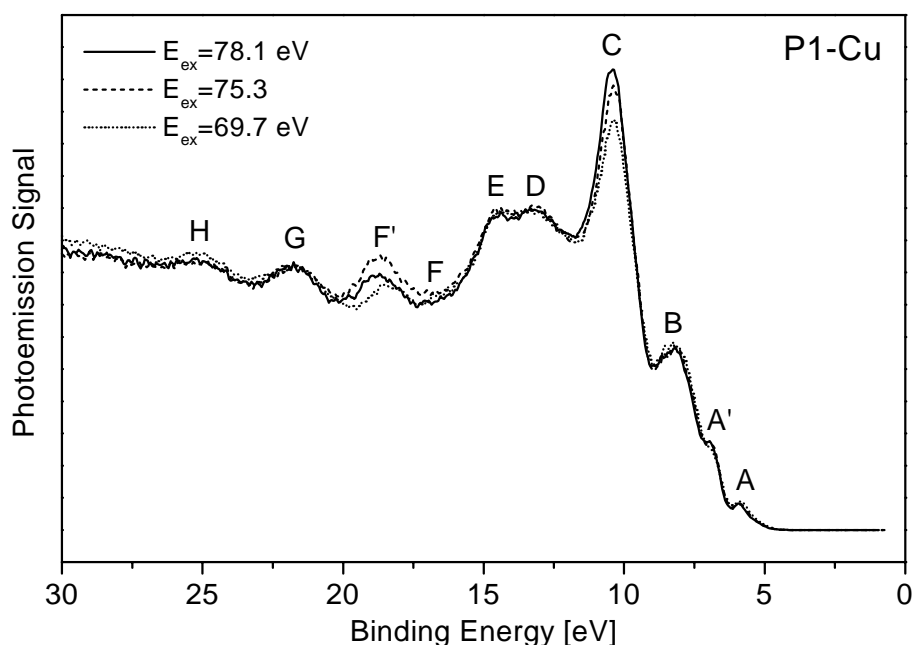

Fig. 5.1-6 Photoemission spectra of the P1-Cu compound for 69.7, 75.3 and 78.1 eV excitation energy. The intensity of band C (containing contributions from Cu3d direct emission) has an increase relative to the ligand features in the spectrum at the increase of the excitation energy, in the photon energy range applied in the present experiments. Feature F' shows a resonant behavior.

Evolution of the Photoemission Features as a Function of the Ligand Size

In order to evaluate the changes induced in the photoemission features by the variation of the molecular size, the spectra for all Cu compounds in the series, obtained for 70.7 eV excitation energy, are displayed in Fig. 5.1-7. For clarity, the photoemission curves are vertically displaced with respect to each other. Due to the fact that the P3-Cu film was obtained by a wet chemical method, its spectrum is less resolved as for the sublimed films. Yet it fairly well reproduces the characteristic photoemission features. The P3-Cu spectrum is more difficult to interpret as this molecule contains phenyl instead of tert-butyl as substituent. Furthermore the corresponding metal-free spectrum is not available.
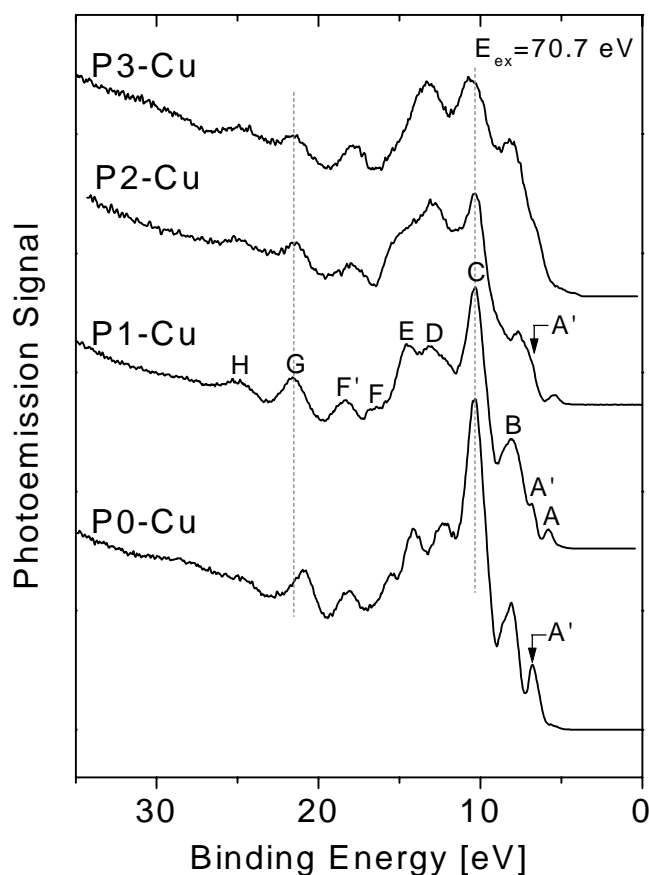

Fig. 5.1-7 Photoemission spectra of the copper porphyrazines in the series obtained for 70.7 eV excitation energy.

As expected, the features containing benzene contributions increase considerably relative to the Cu3d main peak at the extension of the ligand. The binding energies of the Cu3d main peak are identical for the first three compounds in the series. Peak C is

considerably broader for P3-Cu, probably due to the additional ligand signal and also to the preparation method. For the latter it is difficult to distinguish copper from ligand contributions. Hence, in case of P3-Cu the estimation of binding energies for the copper features in the spectrum is not possible.

The peak derived from the HOMO of the molecule/peak A' appears at approximately identical binding energy for P0-Cu and P1-Cu. Roughly at the respective binding energy, a shoulder is present in the P2-Cu spectrum. It is proposed that this shoulder is in fact the feature derived from the HOMO of P2-Cu, which is not better distinguishable due to overlapping ligand features at that position.

Concerning the evolution of the ligand peaks, one observes in Fig. 5.1-7 that bands H and G have the same binding energy for P1-Cu, P2-Cu, and P3-Cu which is expected considering that they are mainly determined by the benzene units. For P0-Cu, similarly to the case of metal-free complexes, band H is considerably less pronounced, and band G is shifted by approximately 0.65 eV towards lower binding energies. Band D is found at the same position for P1-Cu and P2-Cu (and perhaps also in P3-Cu), but it has a lower binding energy (by ~0.4 eV) in P0-Cu. Again, this is consistent with the significant benzene character of this band for P1-Cu and P2-Cu. For the first three compounds in the series, peak E shifts to larger binding energies at the increase of the ligand size. This perhaps comes from the overlap between metal and ligand contributions. Similar to the metal-free compounds case, band B does not shift at the addition of benzo-units for P0-Cu and P1-Cu, most probably due to the important contributions of the meso-nitrogens to it. It is found at slightly lower binding energies for P2-Cu.

The band A, which arises from the HOMO-1 (ligand character), in the case of P1-Cu and P2-Cu, has a similar evolution as for the metal-free compounds. For P3-Cu this is difficult to infer due to the fact that band A is not resolved in the spectrum.

In order to compare the binding energies of bands A and A' for the different compounds in the series, a blow-up of the valence region in the 0-10 eV binding energy range is presented in Fig. 5.1-8. These spectra are identical with those shown in Fig. 5.1-7. The spectrum of the P3-Cu compound is omitted, as it is not conclusive for this purpose.

Feature A is well resolved in the spectra of P1-Cu and P2-Cu but not for the P0-Cu compound. However, a more thorough analysis of the band found at about 6.8 eV binding energy in P0-Cu spectrum reveals an asymmetric shape of this feature, with a low binding energy tail. Taking this into account and, in addition, the fact that HOMO is well resolved for P0-H$_2$, it is concluded that the asymmetric feature found at ~6.8 eV binding energy in

the P0-Cu spectrum includes both HOMO (metal character) and HOMO-1 (ligand character) contributions.
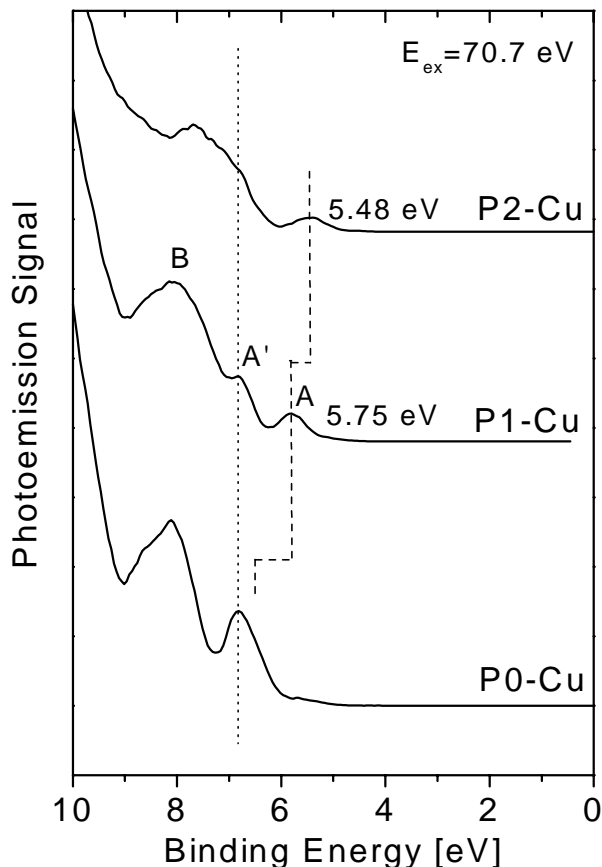

Fig. 5.1-8 Photoemission spectra of the valence region for P0-Cu, P1-Cu and P2-Cu compounds (expanded from Fig. 5.1-7). Energies for band A are labeled for P1-Cu and P2-Cu. A ±0.07 eV uncertainty must be considered for the given values. The position of band A in the case of P0-Cu can not be identified unequivocally due to peak overlap.

For extracting the position of bands A and A', both the P1-Cu and P0-Cu spectra were fitted with a sum of four Gaussians in the 4.0-9.4 eV binding energy region. The contributions giving rise to band A are similar in P0-Cu and $P0-H_2$ (HOMO in $P0-H_2$ has identical composition with HOMO-1 in P0-Cu). Therefore, for the fit of the P0-Cu spectrum, it was imposed the condition to have the same widths of band A as in the $P0-H_2$ spectrum. The result of the performed fitting procedure is shown in Fig. 5.1-9. The binding energy of the peak A/HOMO-1 in P0-Cu was determined to be 6.50±0.1 eV. For peak A', one obtains in this way 6.85±0.1 eV for P0-Cu and 6.72±0.1 eV for P1-Cu.
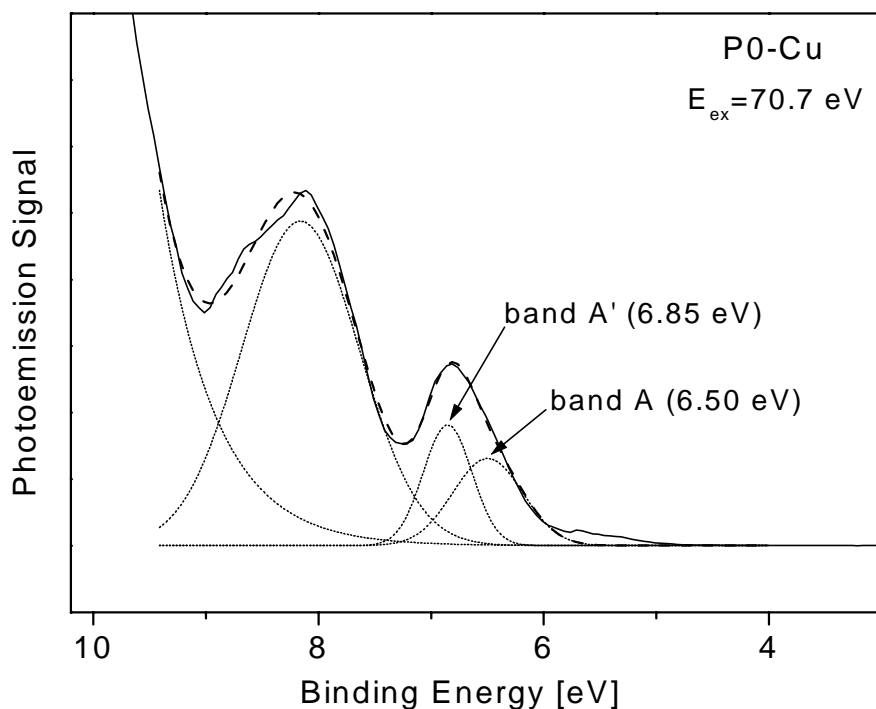
Fig. 5.1-9 The result of fitting the 4.0-9.4 eV binding energy range for the P0-Cu spectrum. It was concluded that the feature found at about 6.8 eV binding energy includes both peaks A/HOMO-1 and A'/HOMO. The binding energy of feature A for P0-Cu was determined to be 6.50±0.1 eV.

As for the metal-free compounds, the binding energy of feature A decreases with increasing number of benzo-units in the molecule. The determined values are: 6.50±0.1 eV for P0-Cu, 5.75±0.07 eV for P1-Cu and 5.48±0.07 eV for P2-Cu. In going from one molecule to the next one in the series, one observes that the larger difference in the binding energy of peak A is between P1-Cu and P0-Cu. This again confirms that the interactions induced by benzene, which determine the destabilization of the a_{1u} orbital, are stronger for the inner ring of benzo-units directly surrounding the porphyrazine core, and become weaker for the outer rings [OCP96].

Table 5.1-1 summarizes the obtained binding energies of feature A (ligand character) relative to the vacuum level in the Cu compounds series along with those obtained for the corresponding metal-free complexes. It is noted that the binding energy of feature A for these Cu compounds is by 0.07-0.15 eV smaller than in the corresponding metal-free complexes. The relative differences in binding energy of peak A in going from one molecule to the other in the Cu series are nearly the same as in the H_2 series case.

Compound	BE for feature A(ligand character)
P0-Cu *P0-H$_2$*	6.50 *6.57*
P1-Cu *P1-H$_2$*	5.75 *5.9*
P2-Cu *P2-H$_2$*	5.48 *5.61*

Table 5.1-1 Binding energy of feature A (ligand character) relative to the vacuum level for copper compounds in the series together with the values obtained for the metal-free complexes (written in italics). All the values are given within ±0.07 eV error range, except for P0-Cu where the uncertainty is ±0.1 eV. Note that the same orbitals contribute to feature A in a copper- and in its corresponding metal-free compound.

5.2 Photodegradation Effects

The influence of synchrotron radiation exposure on the samples was also investigated in case of the above Cu compounds.

Similar to the situation for the metal-free complexes, in the Cu series P0-Cu is the most sensitive material from this point of view, showing certain changes in the photoemission spectrum after the time required for recording even the first spectrum. This is illustrated in Fig. 5.2-1 where the photoemission spectra obtained for different exposure times with 75.8 eV photons are displayed. The spectra in the figure are normalized to the background intensity. In Fig. 5.2-1(a) the spectra are vertically displaced for gradually perceiving the effects of radiation on this material. In addition, in Fig. 5.2-1(b) two photoemission curves are plotted on top of each other, corresponding to short and long exposure, respectively (the spectra were taken from the same spot that was different from the one employed in part (a) of the figure). Photodegradation results in broadening and smearing out of all peaks. Feature F', which contains contribution from the Cu satellites, is also found to shift. Similar to the P0-H$_2$ case, for P0-Cu photodegradation is accompanied by a change in color of the exposed spot, which turns from initially dark violet (for a thick film) to a light color.

For P1-Cu the effect of synchrotron light is less pronounced and the photodegradation rate is considerably lower as compared to P0-Cu. Still, a broadening and

smearing out of the photoemission features is observed due to the synchrotron light exposure (as shown in Fig. 5.2-2).
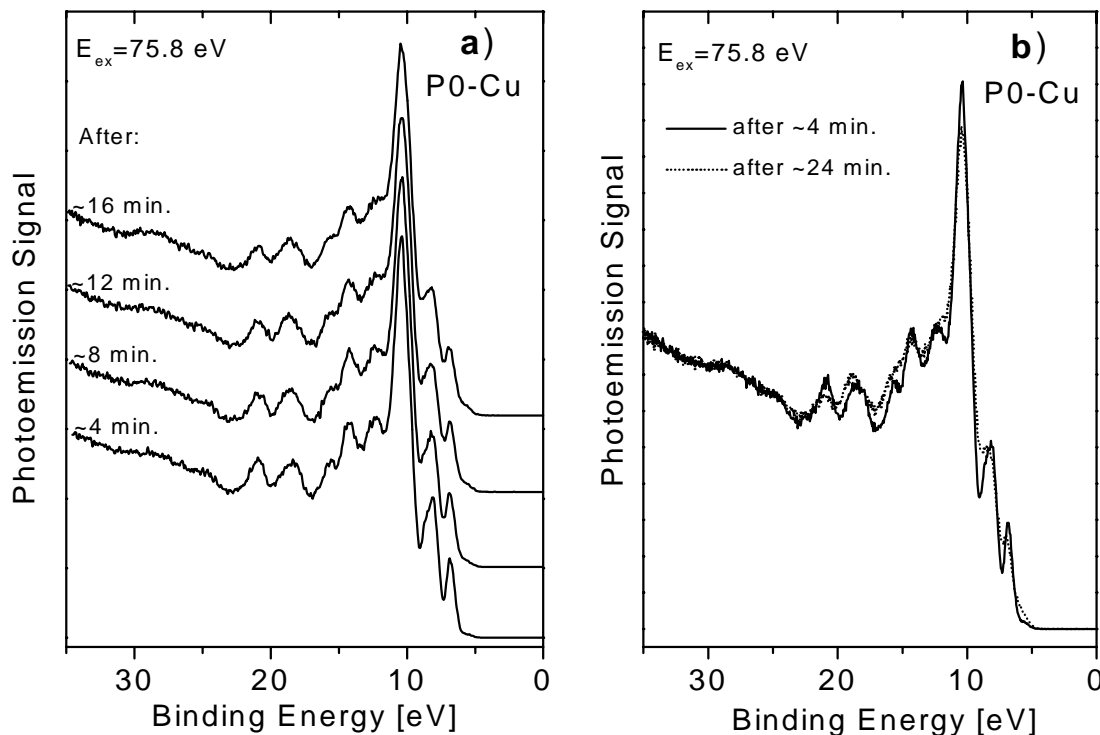

Fig. 5.2-1 Photoemission spectra of P0-Cu after various synchrotron radiation exposure times.

Even smaller synchrotron radiation exposure effects are observed for the P2-Cu compound. No photodegradation effects were detected for the P3-Cu films. This is true for both preparation procedures: UHV evaporation (films containing decomposition products) and wet chemical method.

The nature of the light-induced processes that give rise to the described changes of the photoemission features was not investigated. For the present experimental purpose, the extent of photodegradation is important for a meaningful analysis and comparison of the data. Certainly, a consequence of the experiments was to make sure that during the measurements the irradiated spots on the sample were systematically changed in order to minimize the radiation-induced damage.
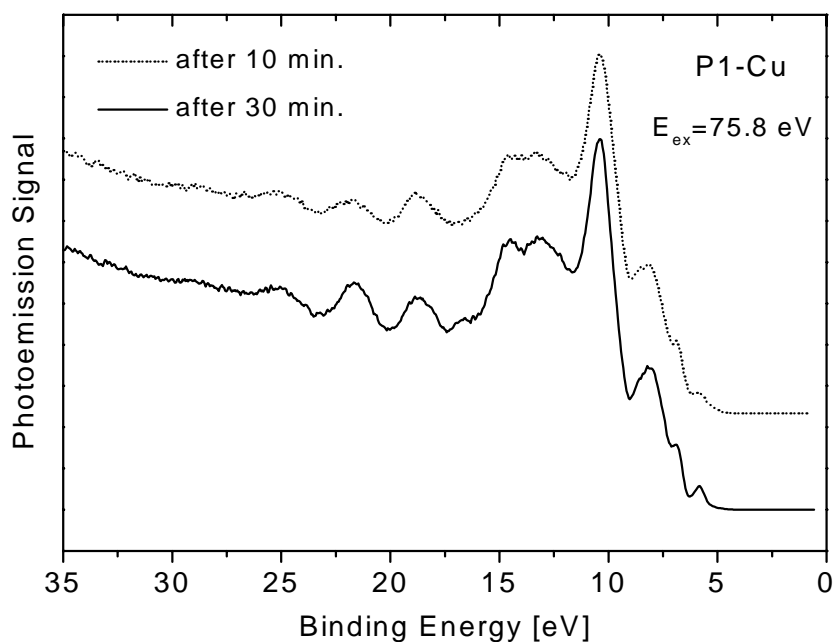
Fig. 5.2-2 Photoemission spectra of P1-Cu upon various synchrotron radiation exposure times.

5.3 Insights from a Study of Copper Satellites

The Cu satellites between ~15.5 and ~19.5 eV, observed in Cu-phthalocyanine (CuPc) spectra similar to those presented in the first section of this chapter, were initially considered to correspond to a $3d^8 4s^2$ final state configuration of Cu [IKC80]. In that case it was assumed that Cu in CuPc can be treated as quasiatomic. To our knowledge, no other studies of the Cu valence satellites in CuPc or analog organic molecules have been reported.

Grioni et. al [GGS89] proved by XAS (X-ray Absorption Spectroscopy) studies that Cu is in the nominal Cu^{2+} ionization state in CuPc. In CuPc the Cu site has D_{4h} symmetry, as it is also the case in copper dihalides. In compounds containing divalent copper it is considered that the copper has a $3d^9$ ground state with a small contribution from $3d^{10}\underline{L}$, where $\underline{L}$ denotes a hole in the ligand. Thus, the attributed final configurations for the main line and the satellite in the valence band are $3d^9\underline{L}+3d^{10}\underline{L}^2$ and $3d^8$, respectively [LWH81]. Such investigations have been done for copper dihalides [LWH81] and CuO [GTE88], which have an open d shell.

However, the Cu2p satellites in CuPc were subject of several experimental [KTI94] and theoretical papers [CDF94] and analogies were made to CuO or copper dihalides.

72

As shown in Chapter 1, the presence of the satellites at the ionization of Cu2p, Cu3s, or Cu3p levels of dihalides was explained by the existence in each of these cases of a well-screened state (main line, $\underline{c}3d^{10}\underline{L}$) and of an unscreened one (satellite, $\underline{c}3d^9$) [LWH81]. Here $\underline{c}$ and $\underline{L}$ indicate that there is a hole in the copper c core level and the ligand valence state, respectively.

For the 2p ionization, the processes which lead to the appearance of the main line and the satellite can be seen in the following way: Upon 2p photoionization, the Cu3d level in the divalent copper compounds (which is sensed as an empty acceptor level) is pulled down below the ligand p orbital by the attractive Coulomb core-hole potential. The ligand p orbital is not affected by the copper core-hole potential [KTI94]. If the photoelectron leaves the copper compound slowly enough, the Cu3d hole is transferred to the ligand p orbital. In other words, a shakedown core-hole state in which the empty acceptor level is filled by charge transfer from the ligand becomes a charge-transfer screened core-hole state [Ohn2001]. If the photoionization of the 2p electron is sufficiently fast, the Cu3d hole remains in the Cu3d atomic orbital with a finite probability after the photoionization of the 2p electron, so no charge transfer from the ligand to the Cu3d orbital takes place. Although the real photoionization process is intermediate between these two limits, they describe suitably the XPS spectra of divalent copper compounds [KTI94]. It was also shown that the charge transfer core-hole screening depends on the ratio between the charge transfer rate and rate of change in separation energies between the acceptor and ligand/donor level. The latter is related to how fast the photoelectron leaves the system upon ionization [Ohn2001].

The central Cu is formally divalent in CuPc and its site has also D_{4h} symmetry. Thus, the interpretation of the main line and the satellite in the photoemission spectra of CuPc is analogous to those of copper dihalides compounds, where Cu is in the nominal Cu^{2+} state.

In the following, the physical processes governing the appearance of satellites and main line in the valence and core levels regions for CuPc will be discussed referring to the relevant energy levels. The energy level diagram will be regarded as being composed from the bare macrocycle Pc^{2-} levels interspersed with the Cu^{2+} ones. For Cu compounds with a nominal $3d^9$ configuration in the ground state, the ligand p level is usually deeper than the Cu3d level and the valence hole exists in the 3d orbital [KTI94]. In CuPc, the $Cu\,d_{x^2-y^2}$ orbital has a single occupancy and the ligand $N_p b_{1g}$ level is the HOMO of the Pc^{2-} dianion [RoB94]. The a_{1u} ligand macrocycle orbital and the other Cu3d orbitals are found even

deeper. With the above mentioned considerations, the energy level diagram for Cu^{2+} and Pc^{2-} can be drawn as shown in Fig. 5.3-1.

$$Cu^{2+} \qquad Pc^{2-}$$

$$b_{1g}(d_{x^2-y^2}) \quad \text{——}$$

$$\text{——} \; N_p b_{1g}$$

$$\text{——} \; a_{1u}$$

$$e_g, \, b_{2g}, \, a_{1g} \; \{\equiv\equiv\equiv$$

Fig. 5.3-1 Important energy levels for Cu^{2+} and Pc^{2-} dianion in CuPc.

Valence region

As shown in the first part of this chapter, according to theoretical calculations the direct emission from the HOMO of CuPc (b_{1g} molecular orbital having $Cu\,d_{x^2-y^2}$ and N_p character) gives rise to contributions at the position of feature A' in the photoemission spectra. In our opinion its low binding energy suggests that this corresponds to a screened final state for copper: we propose that at the ionization, charge is transferred from the ligand (N_p lone pair b_{1g} level) to the $Cu\,d_{x^2-y^2}$ orbital. This appears more likely than a two-hole $Cu\,d_{x^2-y^2}$ state. Thus, the current picture is that part of feature A' corresponds to a final configuration of the system with one hole in the $Cu\,d_{x^2-y^2}$ orbital and another hole in the ligand (N_p lone pair).

We interpret that at the other copper d-like ionizations, from $e_g(d_{zx},d_{yz})$, $b_{2g}(d_{xy})$ or $a_{1g}(d_z^2)$, the screening of the hole by an electron transferred from the ligand $N_p b_{1g}$ orbital into $Cu\,d_{x^2-y^2}$ orbital gives rise to the features observed at the position of band C in the spectra. The final configuration corresponding to these contributions in feature C is accordingly with a hole in one of these d orbitals mentioned before, and a hole in the ligand ($Cu\,d_{x^2-y^2}$ is filled by charge transfer). The satellite features correspond to the case when no charge transfer occurs at the ionization of d-like e_g, b_{2g}, a_{1g} orbitals and the final configuration associated with them is one hole in one of the e_g, b_{2g}, a_{1g} orbitals and one hole in the $Cu\,d_{x^2-y^2}$ orbital.
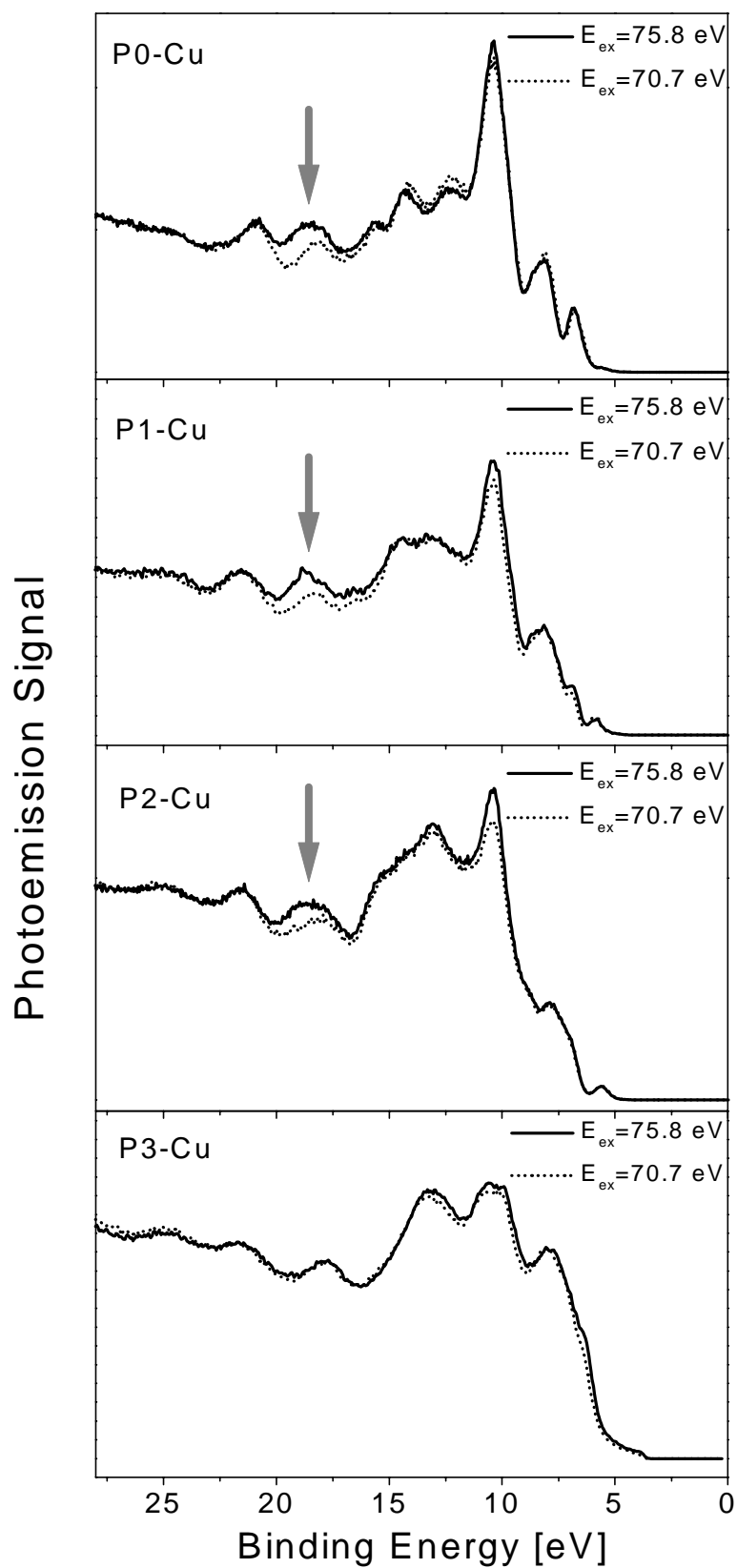
Fig. 5.3-2 Photoemission spectra for thin films of the Cu porphyrazine compounds at 70.7 and 75.8 eV photon energy. Arrows mark the Cu3d satellite peaks near 18 eV binding energy.

It implies that the satellite features observed in the valence region of CuPc correspond to a $3d^8$ final configuration of Cu in the molecule. This explains the presence of the Cu valence satellite in the spectra, for each excitation energy used in the present experiments (as can be inferred from the comparison of the CuPc and H_2Pc spectra).

The spectra obtained for 75.8 and 70.7 eV photon energy are presented in Fig. 5.3-2 for all Cu-porphyrazines in the series. Arrows mark the positions of the Cu satellite peaks. Near 75 eV excitation energy an increase of the Cu satellite emission is observed for CuPc, P0-Cu, P1-Cu and P2-Cu. The effect does not appear for P3-Cu.
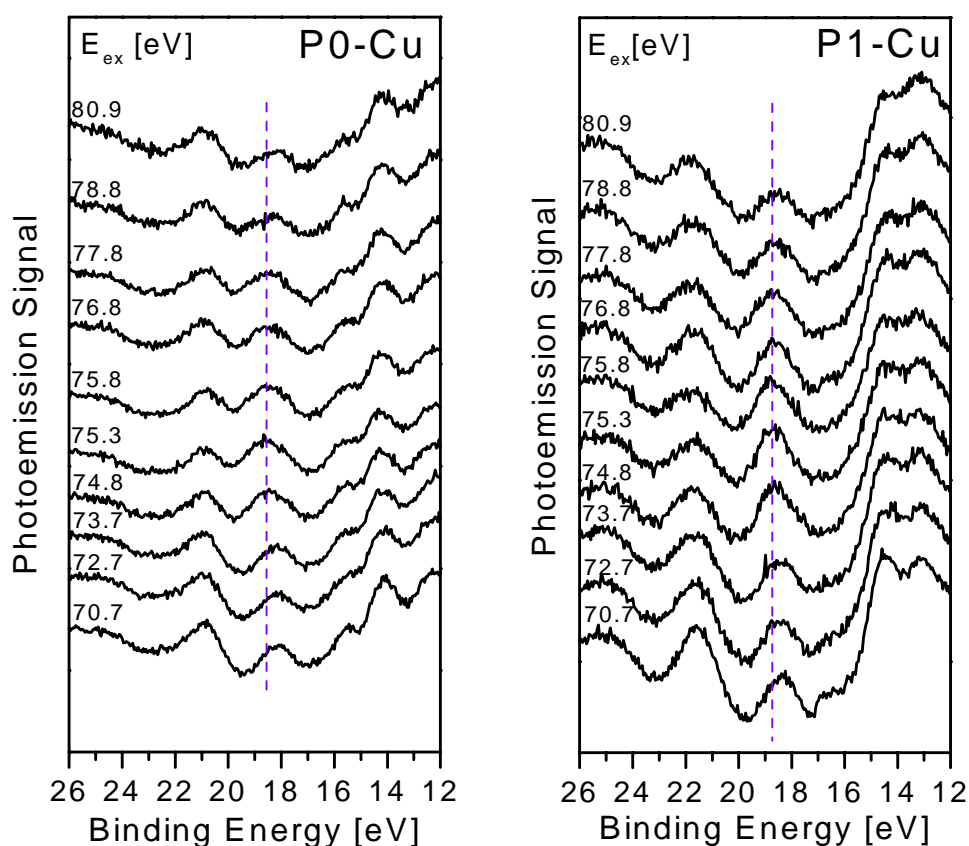
Fig. 5.3-3 Blow-up of the Cu satellite region for P0-Cu and P1-Cu. The spectra were obtained at several excitation energies around resonance. The position of the satellite peak at resonance is marked.

The enhancement of Cu satellite peaks for P0-Cu and P1-Cu may be directly seen in Fig. 5.3-3 where the photoemission spectra taken at several excitation energies are displayed. The spectra have been normalized to the ligand feature H and then vertically shifted for better observing the variations in satellite intensity. One can note that the

maximum satellite intensity is reached at about 75 eV excitation energy for both compounds. The same is also true for P2-Cu and CuPc. Since the behavior of P0-Cu, P1-Cu, and P2-Cu resembles very much that of CuPc, it results that these molecules have similar electronic structure to that of CuPc. Thus, the energy level diagram for each of these molecules is analog to that of CuPc.

We interpret that, like for other divalent copper compounds, the satellite enhancement at about 75 eV photon energy is related to the 3p-3d transition in Cu, more precisely to the transition from one of the 3p orbitals into the $Cu\, d_{x^2-y^2}$ orbital. In the current picture the $Cu\, 3p$-$Cu\, d_{x^2-y^2}$ excitation is accompanied by an Auger decay from one of d-like $e_g(d_{zx},d_{yz})$, $b_{2g}(d_{xy})$ or $a_{1g}(d_z^2)$ copper orbitals, with emission of an electron found in $Cu\, d_{x^2-y^2}$. Fig. 5.3-4 sketches this process in a very simplified manner. Consequently, the final configuration reached in Cu at resonant excitation is $3d^8$, with one hole in one of the d-like $e_g(d_{zx},d_{yz})$, $b_{2g}(d_{xy})$ or $a_{1g}(d_z^2)$ copper orbitals and one hole in $Cu\, d_{x^2-y^2}$, which is the configuration of the Cu valence satellite. The same is also true if the $Cu\, 3p$-$Cu\, d_{x^2-y^2}$ excitation is accompanied by the Auger decay of an electron from $Cu\, d_{x^2-y^2}$ with emission of one from the $e_g(d_{zx},d_{yz})$, $b_{2g}(d_{xy})$ or $a_{1g}(d_z^2)$ orbitals. We conclude that these mechanisms lead to the enhancement of the satellite features when the condition for $Cu3p$-$Cu\, d_{x^2-y^2}$ excitation is fulfilled. Around this photon energy the direct photoemission is in resonance with the Auger electron emission, thus coherent superposition of the directly photoemitted electrons and Auger electrons can take place.

In P0-Cu, P1-Cu, and P2-Cu spectra no indication of a 3p-4s resonance is found.

The fact that this is a true resonance and not a non-coherent superposition of the photoemission signal with the Auger emission is suggested by several characteristics of the process. $Cu\, d_{x^2-y^2}$ appears to be a localized orbital, the localization of the intermediate state favoring a true resonant process [LGL95]. In addition, the satellites are found roughly at constant binding energy. The constant binding energy of the enhanced feature is a fundamental characteristic of the resonant photoemission [MWK97, GCP2000, QAA95].
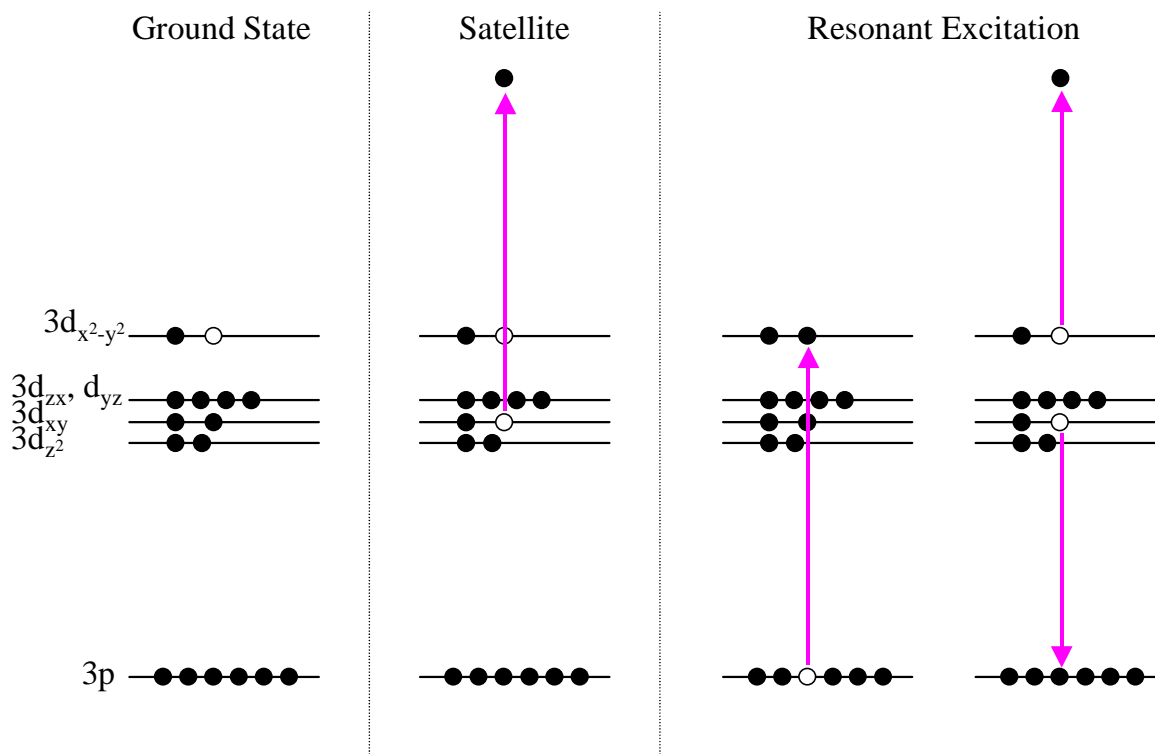
Fig. 5.3-4 Sketch of the copper ground state, of the final state corresponding to the satellite and of the final state reached after 3p-3d resonant excitation, in the case of CuPc and of copper porphyrazines with incomplete d shell. Considered here is the particular case when the satellite corresponds to the ionization of $3d_{xy}$ orbital and accompanying the resonant excitation, the Auger decay occurs from $3d_{xy}$ with the emission of an electron found initially in $3d_{x^2-y^2}$. For simplification, the spin-orbit splitting of Cu 3p level after 3p hole creation is neglected.

The spectra displayed in Fig. 5.3-3 show that the satellite peak (F') is shifted by about 0.3-0.4 eV towards higher binding energies for photon energies close to the resonance maximum as compared to the 70.7 or 80.9 eV off-resonant photon energies. For the extreme off-resonant energies (70.7 and 80.9 eV), the peak is found at identical position. The resonant enhancement is well visible for the 73.7-78.8 eV excitation energy range while the shift of the satellite peaks is much smaller (maximum 0.4 eV as previously mentioned). For CuO it was established that the valence band satellite has a singlet and a triplet component, with the singlet found at higher binding energy than the triplet. The singlet resonates more strongly than the triplet [ETS90, TCG91]. Therefore, we assume that the small shift towards higher binding energies for excitations around the resonance maximum in copper porphyrazines can be explained based on the different enhancements of the singlet and triplet component of the satellite. In addition, it should also be considered that for copper porphyrazines the satellite peaks are found on the top of a strong ligand signal (large ligand contributions are also found at the position of bands F and F').

In order to determine the overall dependence of the Cu valence satellites on photon energy, the ratio between an area which included the satellite peaks and an area including only ligand features, as depicted in Fig. 5.3-5, is considered. By making these ratios (normalization), the influence of different synchrotron intensities on the spectra is eliminated. However, this is not a quantitative evaluation of the satellite intensity variation with photon energy (the ratio is between an area including satellite and ligand contributions and an area including only ligand signal), but we trust that it gives a correct qualitative description of the resonance.
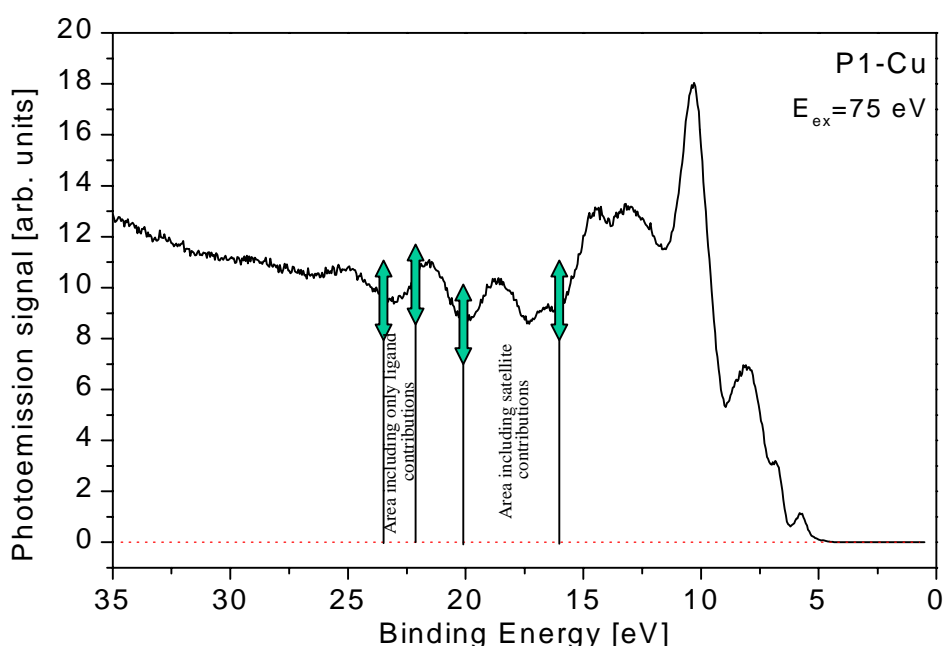
Fig. 5.3-5 Sketch of the areas used for determining the overall dependence of the Cu satellite intensity on excitation energy.

Fig. 5.3-6 shows the intensity change in the region of Cu satellites (at the position of bands F and F') as a function of photon energy for P0-Cu, P1-Cu and P2-Cu. A curve that has a double-peak structure is obtained. A similar dependence is also obtained for CuPc.

In all cases these data may be well fitted by a superposition of two Gaussian curves of equal widths and with the separation between their centers equal to 2.2 eV. This spacing corresponds to the $Cu3p_{1/2}$-$Cu3p_{3/2}$ splitting. In this light, the doublet is attributed to the excitation of the spin-orbit split components $3p_{1/2}$ and $3p_{3/2}$ of the Cu 3p level.
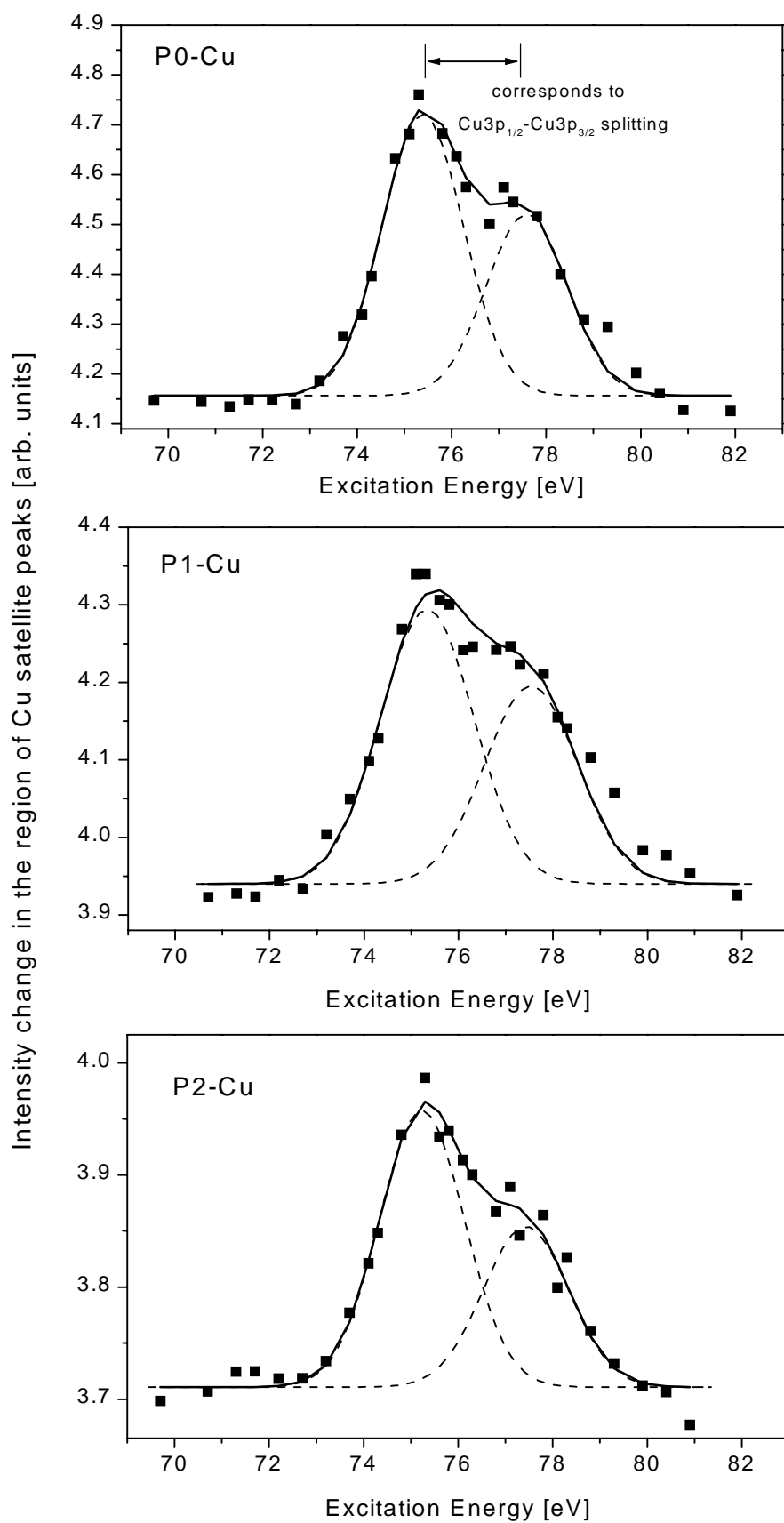
Fig. 5.3-6 The intensity change in the region of Cu satellite peaks as a function of the excitation energy for P0-Cu, P1-Cu and P2-Cu.

For the different copper compounds, no systematic change in the widths of the peaks found by fitting the resonance curve, neither in their position is found.

Considering the way these curves were obtained, it is clear that they do not allow a comparison of the Cu satellite intensity or resonant enhancement between different molecules in the series. This is because both areas used for determining the ratios include the ligand signal.

Since the satellite enhancement involves the 3p-3d excitation, it implies the existence of at least one hole in the 3d (namely $Cu\,d_{x^2-y^2}$) level. Thus, the presence or absence of the satellite enhancement points out an incompletely filled or fully filled 3d shell, respectively. Accordingly, the photoemission data in Fig. 5.3-2 suggest that for CuPc, P0-Cu, P1-Cu, and P2-Cu compounds the Cu configuration in the ground state is nominally $3d^9$, whereas in the largest compound, P3-Cu, Cu is in a $3d^{10}$ formal configuration.

However, in the case of P3-Cu, at excitation energies where the 3p-4s excitation can occur, no clear resonant enhancement of any photoemission feature is observed, even if certain very small intensity variations exist for the feature found at 21.6 eV binding energy. It is interpreted that such enhanced features, which would correspond to a $3d^8 4s^1$ final state, like for Cu_2O [GTE90] or copper halides [ITK86], are not detected for P3-Cu due to the large ligand signal in comparison to the copper one for this molecule.

NEXAFS Measurements

As an alternative approach to investigate the initial state configuration, NEXAFS studies were carried out. The measurements were done on a P3-Cu film deposited by the wet chemical method (which did not show resonant behavior in the Cu satellite found in the valence region) and a P2-Cu film prepared by the same wet chemical method. Fig. 5.3-7 depicts the absorption spectra for the films of P2-Cu and P3-Cu measured at the Cu L_3 edge. The data were normalized at the signal obtained for 945 eV photon energy. The spectra are vertically displaced for clarity. Whereas a strong absorption peak at around 932.5 eV photon energy is found for P2-Cu, this feature is significantly weaker for the larger P3-Cu compound. Such a strong peak is characteristic for Cu compounds in which Cu has a $3d^9$ configuration, being associated to the $2p_{3/2}$ to 3d transition. For the NEXAFS spectra of unsubstituted CuPc, the absorption peak was related to the Cu $2p_{3/2}$-$Cu\,3d_{x^2-y^2}$ transition [CLÅ2001].
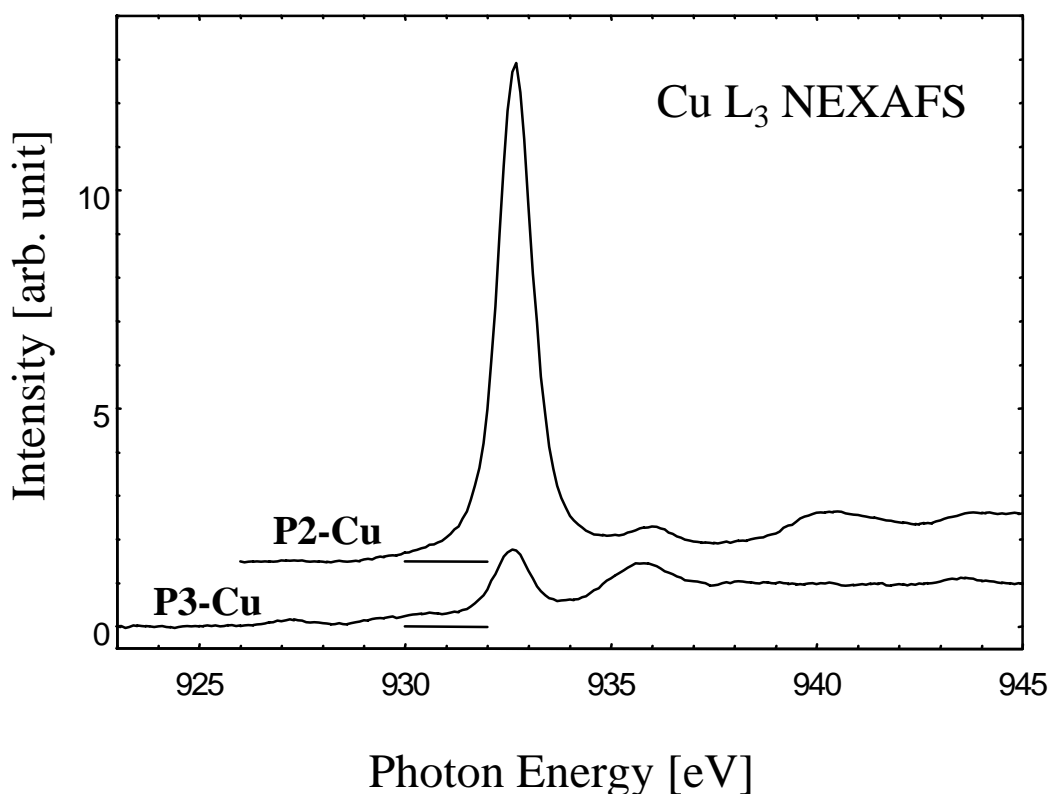
Fig. 5.3-7 NEXAFS spectra for the P2-Cu and P3-Cu compounds. The spectra are vertically translated for clarity.

The different signal intensities for P2-Cu and P3-Cu support the results drawn from the spectra of the valence region, namely that the initial configuration of Cu is different in these two molecules. The absorption edge for the largest molecule, P3-Cu, resembles very much the characteristic data for Cu^I (formally monovalent) or Cu^0 compounds having completely filled 3d shells [GGS89]. Thus, from the NEXAFS measurements it is inferred that in P3-Cu compound the central Cu atom has a full 3d shell ($3d^{10}$).

The resemblance between the P2-Cu NEXAFS spectra and those reported in the literature for CuPc [DPR94, DPR95] confirms that also for P2-Cu the nominal ionization state of the central copper is Cu^{2+}.

XPS Measurements

Further corroboration for the initial state configuration of the central Cu atom in the molecules comes from additional XPS studies with non-monochromatized Al Kα radiation (main excitation energy 1486.7 eV).

Since not each film could be obtained by UHV sublimation, in order to identify the possible influence of the preparation method on the XPS spectra, measurements were performed on both a P2-Cu film prepared by sublimation and on a P2-Cu film obtained by the wet chemical method. The results of the measurements of the Cu2p and N1s core levels

for these P2-Cu films are presented in Fig. 5.3-8. These regions of the spectra contain information about the Cu configuration (and bonding) in the molecule. A Shirley type background was subtracted in case of N spectra while for the Cu spectra a linear background subtraction was performed. The Cu and N spectra were normalized to the corresponding maximum intensity signal and then the spectra were vertically translated for clarity.
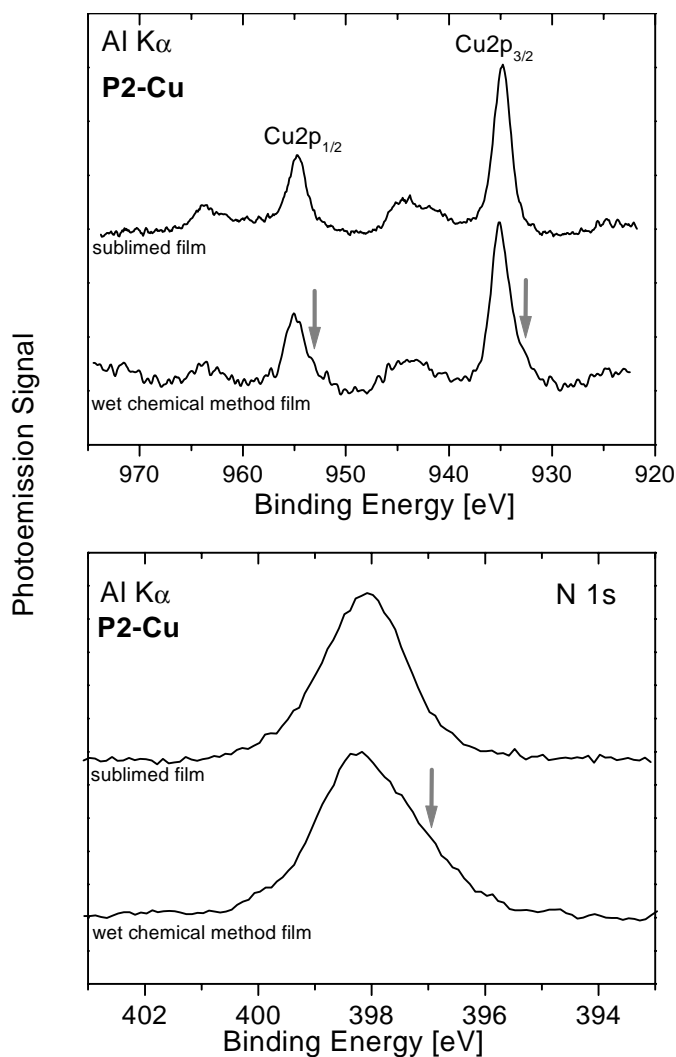

Fig. 5.3-8 XPS spectra at the Cu2p core levels (top) and at the N1s level (bottom) for a P2-Cu film obtained by sublimation in UHV and for a P2-Cu film prepared by wet chemical method.

In these and in the following spectra shown in this section, the binding energy scales were established by defining the C1s peak at a binding energy of 284.2 eV, as determined by Rochet et. al. for the aromatic carbon peak in CuPc [RDR94].

Significant oxygen signal was detected in the case of the ex-situ prepared film but not for the vacuum sublimed one. As can be observed in Fig. 5.3-8, the Cu2p (top) main peaks have a slight shift of about 0.27 eV towards higher binding energy for the ex-situ prepared film as compared with the one obtained by sublimation in UHV. Cu satellite features may be well distinguished, occurring at roughly the same positions for both films. A careful examination reveals that the Cu2p main peaks for the film prepared by wet chemical method exhibit a shoulder on the low binding energy side. This is better observed at the position of $Cu2p_{3/2}$ main line. Also, the ratio between satellites and main line is slightly smaller in case of the ex-situ prepared film compared to the sublimed one. These observations most likely indicate the reduction of some of the central copper atoms due to the interaction with the ambient atmosphere during film preparation.

Yet, since the Cu2p spectra for the two films are quite similar, it can be concluded that this is a minor effect for P2-Cu. The N peak (Fig. 5.3-8 bottom) for the ex-situ prepared film is shifted by 0.12 eV to higher binding energy and has a shoulder as compared to the sublimed one.

From the above mentioned facts it follows that the C, N, and Cu features in the XPS spectra of all molecules in the series may be compared qualitatively. This seems true even if the P3-Cu film can be obtained only by the wet chemical method, showing certain oxygen intrusions.

For all Cu porphyrazines in the series, the XPS spectra of Cu2p lines with a linear background subtraction are shown in Fig. 5.3-9.

The curves are normalized to the $Cu2p_{3/2}$ peak height and vertically displaced for clarity. The peaks observed in all spectra at a binding energy roughly 10 eV lower than for the $Cu2p_{3/2}$ main line are due to the excitation of the sample by the $AlK\alpha_{3,4}$ radiation components. It is noticed that for P0-Cu, P1-Cu, and P2-Cu, broad satellite peaks are present on the high binding energy side of the Cu $2p_{1/2}$ and $Cu2p_{3/2}$ main lines. These type of satellites are characteristic of materials having a copper $3d^9$ configuration in the ground state [GTE88]. As previously mentioned the main line for each of the two split components corresponds to a charge transfer state in which a core hole is screened by the electron transfer from the ligand to Cu3d, being associated with the $\underline{2p}3d^{10}\underline{L}$ final state. The satellites correspond to the unscreened state, being predominantly due to $\underline{2p}3d^9$ final configuration [LWH81]. Here $\underline{2p}$ and $\underline{L}$ indicate that there is a hole in the Cu2p and the ligand valence state, respectively. The binding energies for the $Cu2p_{3/2}$ main line are determined to be 934.9±0.2 eV for P0-Cu, 934.9±0.2 eV for P1-Cu and 934.8±0.2 eV for

P2-Cu, respectively. Therefore, in the error bars limits, the separation between the C1s peak and Cu2p main lines is the same for P0-Cu and P1-Cu. The satellite positions have identical binding energies in the spectra for P0-Cu, P1-Cu and P2-Cu.
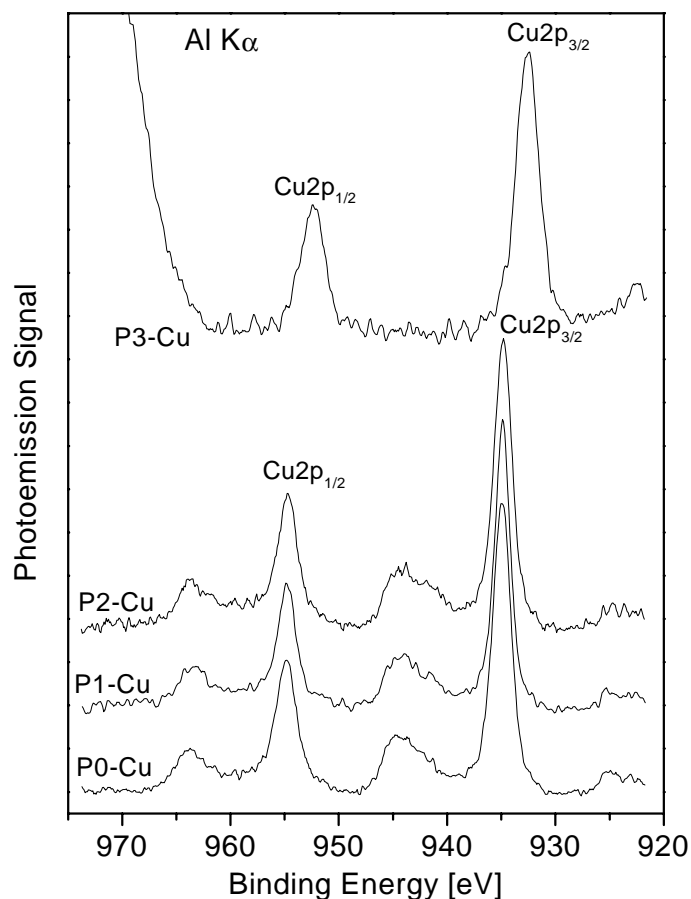

Fig. 5.3-9 Cu2p XPS spectra for the investigated Cu porphyrazines. A linear background subtraction was performed.

The Cu2p XPS spectrum of the P3-Cu compound shows no satellites and one can notice that the $Cu2p_{1/2}$ and $Cu2p_{3/2}$ lines are shifted by about 2.3 eV towards lower binding energies as compared to the other molecules. The $Cu2p_{3/2}$ peak is found at 932.6 eV in this case. The main lines are also broader but this is most probably the result of the preparation method for this film (ex-situ). As remarked in the case of P2-Cu films obtained by sublimation and by wet chemical method, the peaks are broader in the case of the ex-situ prepared film whereas the position of the peaks appears not much affected. As the absence of the Cu2p satellites is generally associated with a filled 3d shell for Cu in the molecule, those XPS results support the result that in P3-Cu the central Cu atom has a nominal $3d^{10}$ configuration.
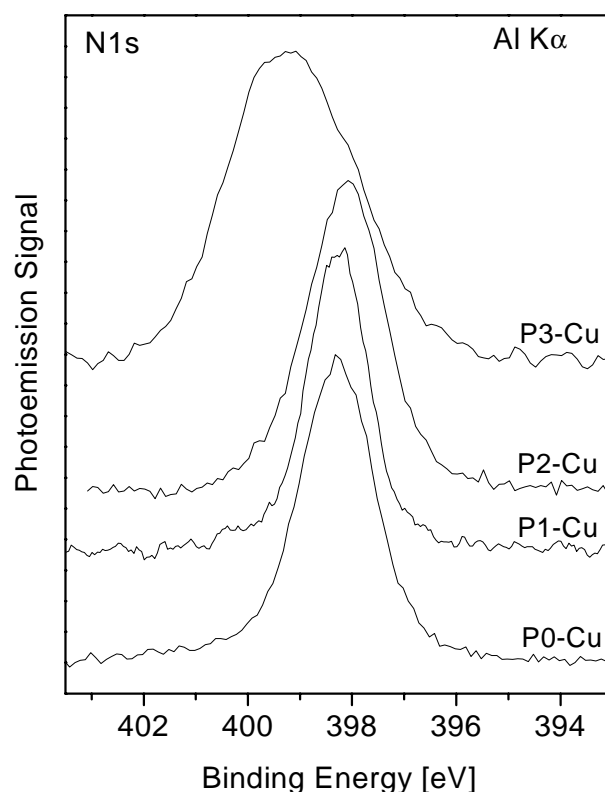
Fig. 5.3-10 XPS spectra of N1s core level for the investigated Cu porphyrazines after Shirley background subtraction

The XPS spectra in the N1s region, after Shirley type background subtraction, are shown in Fig. 5.3-10. The spectra have been normalized at the N1s peak height and then vertically translated for clarity. This peak contains contributions from the pyrrolic and meso-bridging nitrogens [OLR99]. It also includes (at 1.6-2 eV higher binding energy than that of the pyrrole nitrogens peak) a satellite originating from a $\pi \rightarrow \pi^*$ valence excitation associated with the core ionization of pyrrole nitrogens [CRD92, OLR99]. The binding energies determined for N1s after background subtraction are: 398.3±0.2 eV for P0-Cu, 398.3±0.2 eV for P1-Cu and 398.1±0.2 for P2-Cu. The smaller widths appearing for the N1s peak of P1-Cu compound in comparison to P0-Cu and P2-Cu is due to different measurement conditions, namely smaller pass energy used in the experiment.

In case of the P3-Cu compound the situation is dramatically different: the maximum of the N1s peak is found at 399.3±0.2 eV, i.e. the separation between C1s and N1s peaks for this compound is 1 eV larger than for P0-Cu, P1-Cu and P2-Cu. We interpret the shift in binding energy of this peak as due to the $Cu3d^{10}$ configuration in P3-Cu (compared to $Cu3d^9$ in the other copper porphyrazines) and consequently to a distortion in the Cu-N bond. Actually, in the case of Cu_2O, where Cu appears as Cu^+, the binding

energy of the oxygen 1s peak (oxygen is the ligand in that case) was found to be larger by roughly 1 eV than in CuO (where the Cu appears as Cu^{2+}) [GTE88].

However, the N1s peak for P3-Cu is much broader than for P0-Cu, P1-Cu or P2-Cu. This indicates a stronger influence of the preparation method (wet chemical) on the P3-Cu compound than on the P2-Cu one.

To summarize, the XPS measurements show characteristic features of the Cu compounds with nominal $3d^9$ configuration in the ground state for P0-Cu, P1-Cu and P2-Cu and typical core level spectra of Cu compounds with $3d^{10}$ configuration in the ground state for the P3-Cu compound. It is not certain at this point if the $3d^{10}$ copper initial-state configuration in P3-Cu is an intrinsic property of the compound or emerges as the result of the preparation method.

5.4 The Dependence of the Satellites on Ligand Size

Core level and valence level excitations lead to different final states of the system. By comparing the respective XPS and UPS data for the copper porphyrazines, aspects related to the charge transfer processes might be inferred.
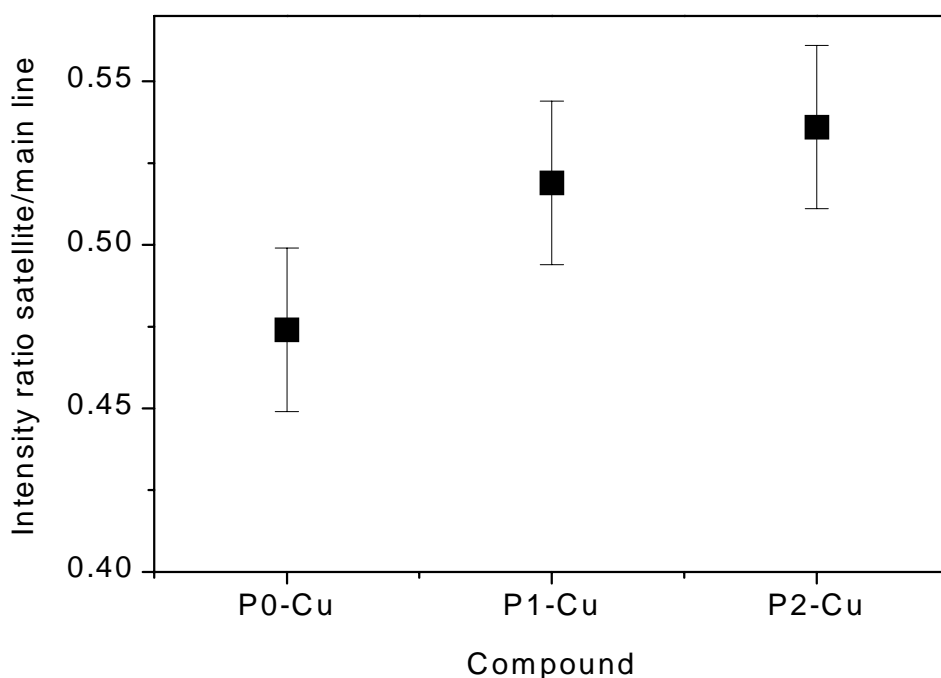

Fig. 5.4-1 The intensity ratio between the $Cu2p_{1/2}$ satellite and main line for P0-Cu, P1-Cu and P2-Cu.

The analysis of the XPS spectra revealed a slight increase of the $Cu2p_{1/2}$ satellite intensity compared to the main line intensity at the extension of the ligand for the first three compounds in the series. The results are displayed in Fig. 5.4-1. The data have been calculated after linear background subtraction from the original spectra.

Fig. 5.4-2 displays the overlapped XPS spectra of P0-Cu and P2-Cu, representing the two extreme cases in terms of $Cu2p_{1/2}$ satellite/main line intensity ratio. The difference in the satellite intensities for these compounds is thus perceptible.
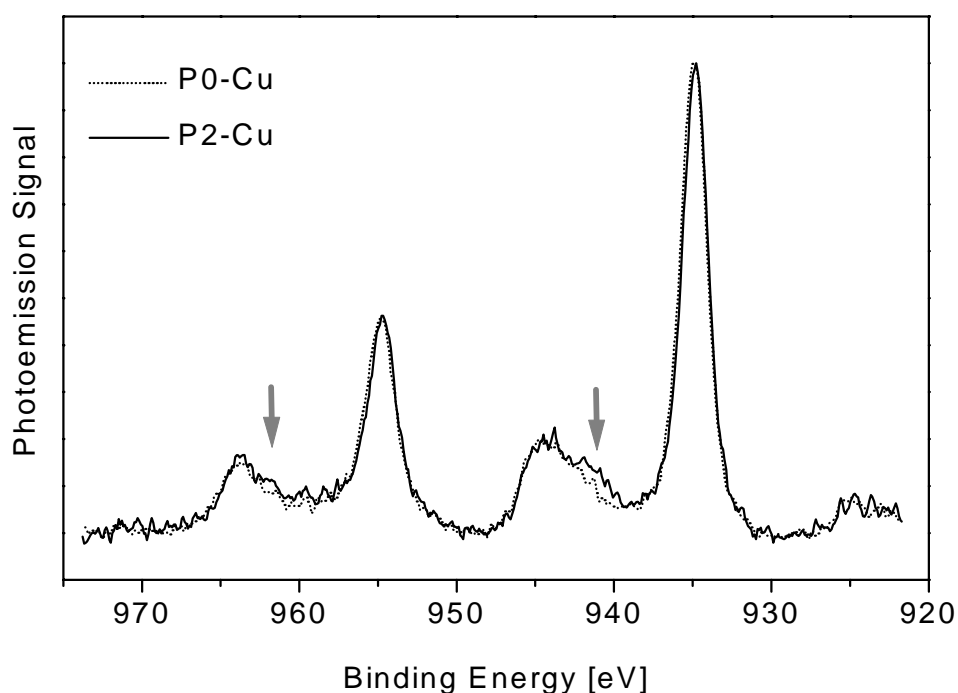
Fig. 5.4-2 The XPS spectra for P0-Cu and P2-Cu in the region of Cu 2p core levels. The difference between the satellite intensities in the two compounds is visible.

For the valence region, in order to determine the intensity ratio between the satellite features and main line, the ligand contributions must be subtracted from the spectra, so that the ratio corresponds entirely to Cu signals. This may be achieved by subtracting the contributions of the corresponding metal-free compound from each Cu-porphyrazine spectrum. Possible effects of the measurement conditions have been avoided by recording both spectra (Cu- and metal-free porphyrazine) at the same photon energies and identical geometrical arrangements.

Due to the different backgrounds in the Cu and metal-free compounds spectra, the overlap of the spectra (necessary for extracting the copper signals) is not possible by simply normalizing them at one of the pure ligand features. This can be seen for the case of CuPc and H_2Pc in Fig. 5.1-3 and for P0-Cu, P1-Cu, P2-Cu and their corresponding metal-free compounds in Fig. 5.1-4. Thus, for extracting the copper contributions, in a first step a background having a linear and a Shirley component was subtracted from all copper and metal-free porphyrazines spectra. As examples for background subtraction procedure, Fig. 5.4-3 and Fig. 5.4-4 display the original spectra, the calculated background and the spectra after background subtraction for P1-Cu and P1-H_2, respectively.

Both spectra were obtained at 73.5 eV photon energy. After background subtraction the resulting spectra were overlapped and the P1-H_2 curve was subtracted from the P1-Cu one. Fig. 5.4-5 shows, for the pair of spectra presented in Fig. 5.4-3 and Fig. 5.4-4, the overlap between P1-Cu and P1-H_2 spectra after background subtraction and their difference signal.
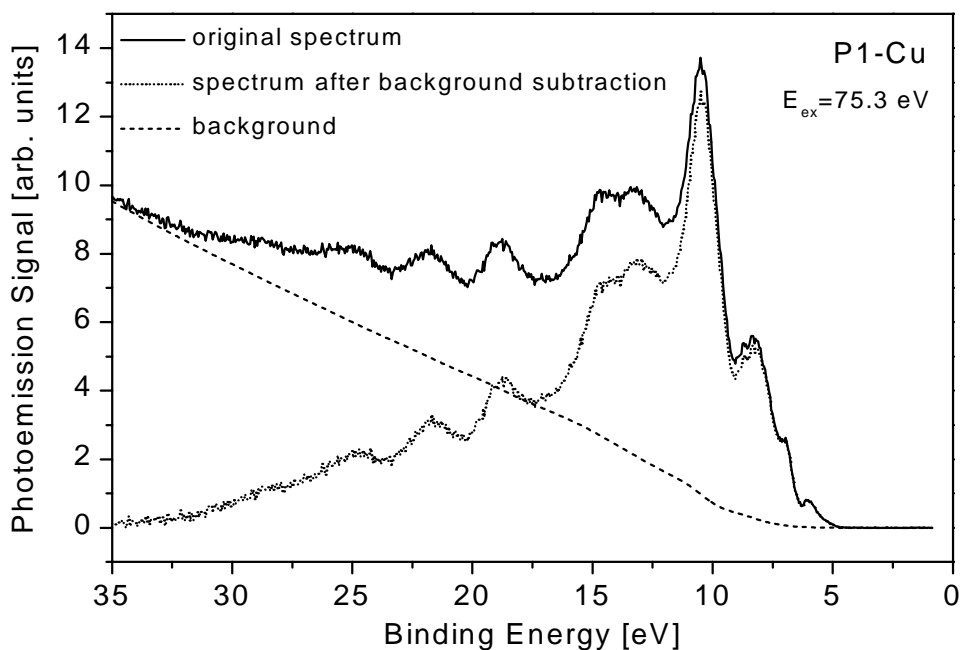

Fig. 5.4-3 The original spectrum, the calculated background, and the spectrum after background subtraction for P1-Cu for 75.3 eV photon energy.
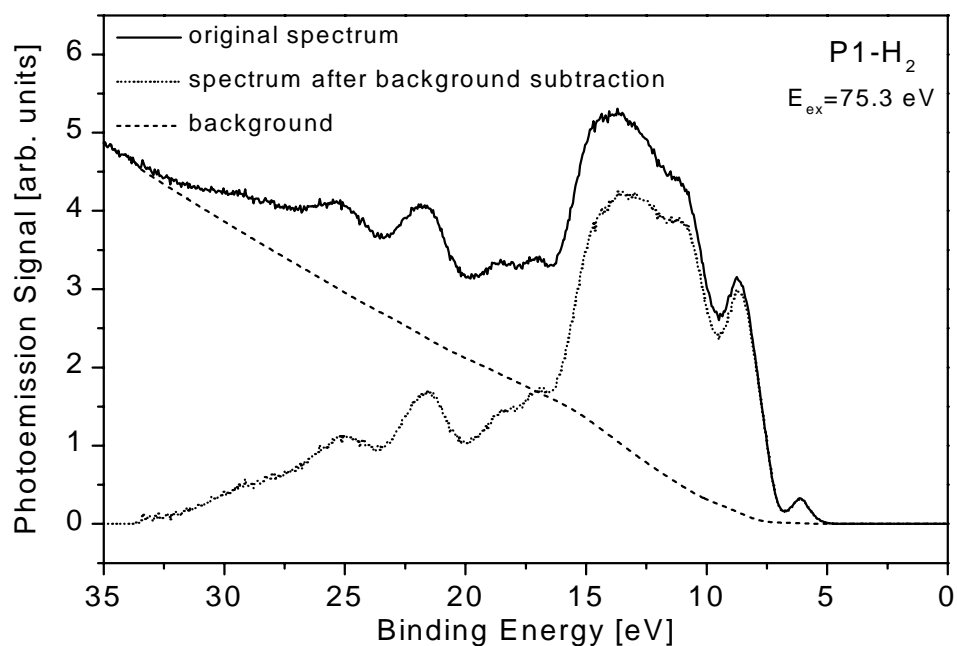
Fig. 5.4-4 The original spectrum, the calculated background, and the spectrum after background subtraction for P1-H$_2$ for 75.3 eV photon energy.
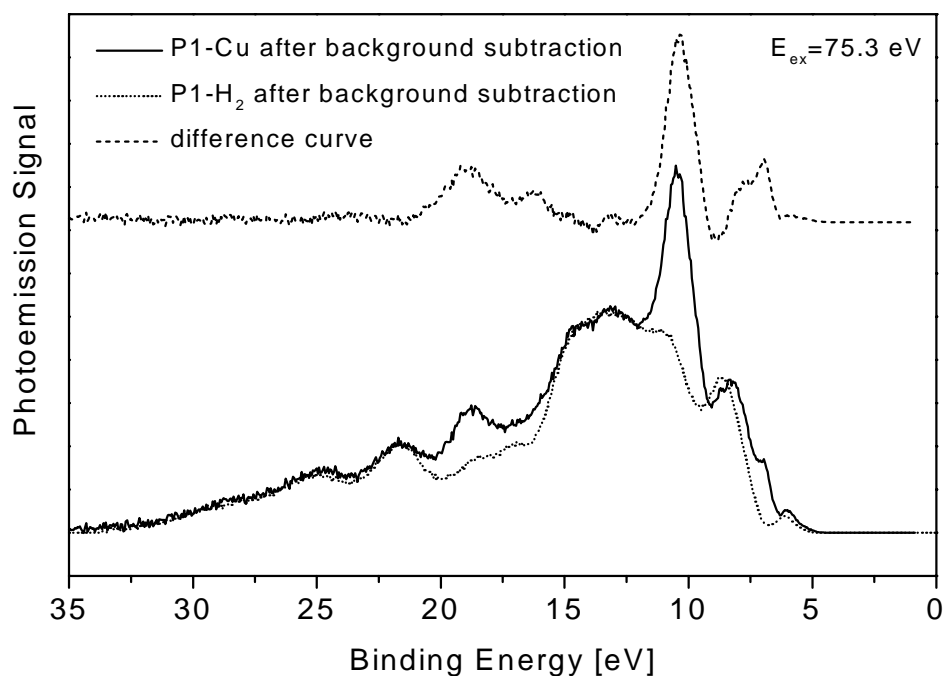

Fig. 5.4-5 The overlap of the P1-Cu and P1-H$_2$ spectra, both after background subtraction, and their difference curve resulted by subtracting the P1-H$_2$ spectrum from the corresponding copper one.
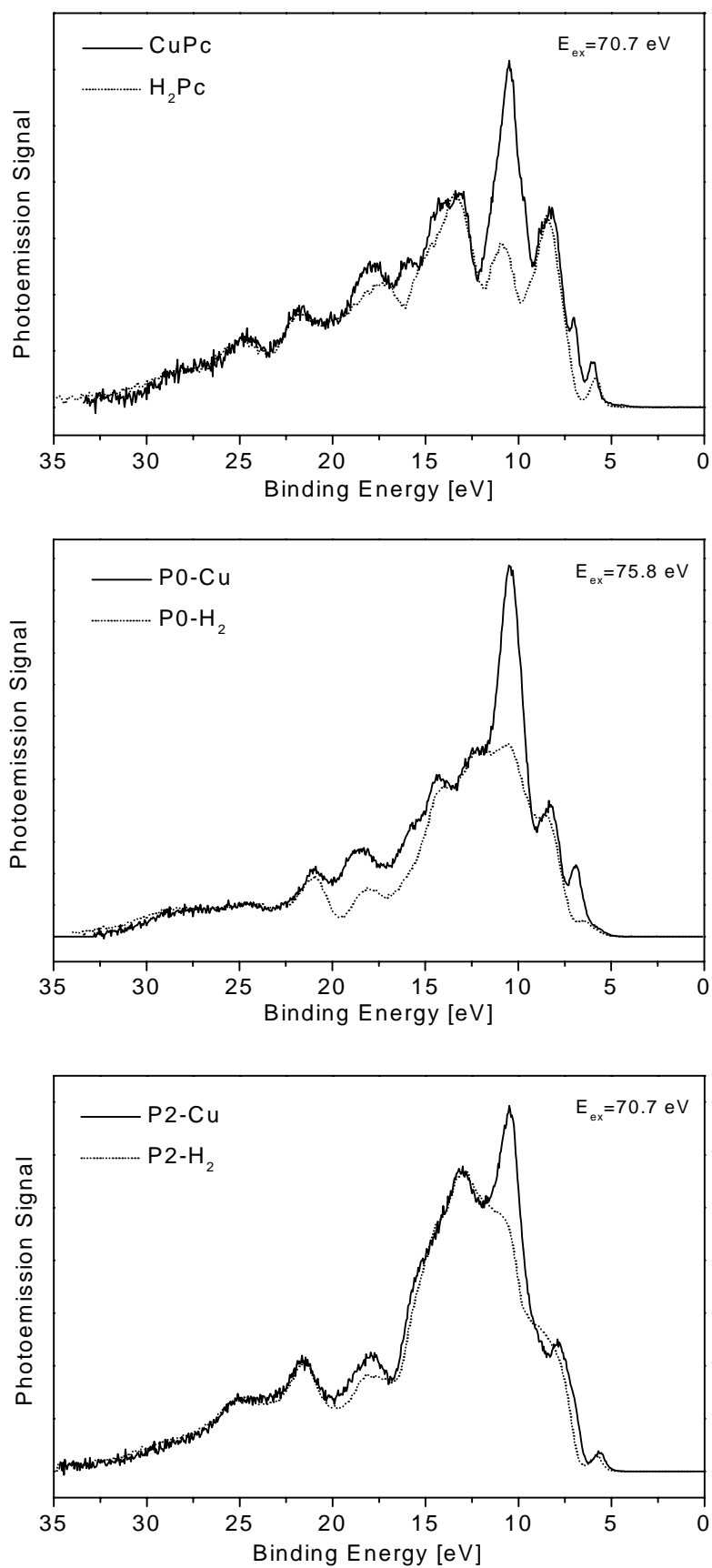
Fig. 5.4-6 The overlap between the spectra of CuPc, P0-H$_2$ and P2-H$_2$ and those of the corresponding metal-free compounds after background subtraction.

Examples of overlapped spectra (after background subtraction) for CuPc, P0-Cu, P2-Cu and their corresponding metal-free compounds are given in Fig. 5.4-6. One can remark that, generally, a reasonable good overlap between the ligand photoemission features of the Cu- and H_2-compounds spectra can be realized after background subtraction. Still, the P0-Cu and P0-H_2 spectra can not always be overlapped at all ligand features, as one can see in the particular case shown in Fig. 5.4-6. In such cases this determines an overestimation of the satellite/main line intensity ratio.

The intensities of the Cu satellite features and main line for a given Cu compound are calculated by integrating the difference curve, obtained after subtraction of the metal-free compound spectrum (with background subtracted) from the Cu one, at the position of satellite and main line, respectively.
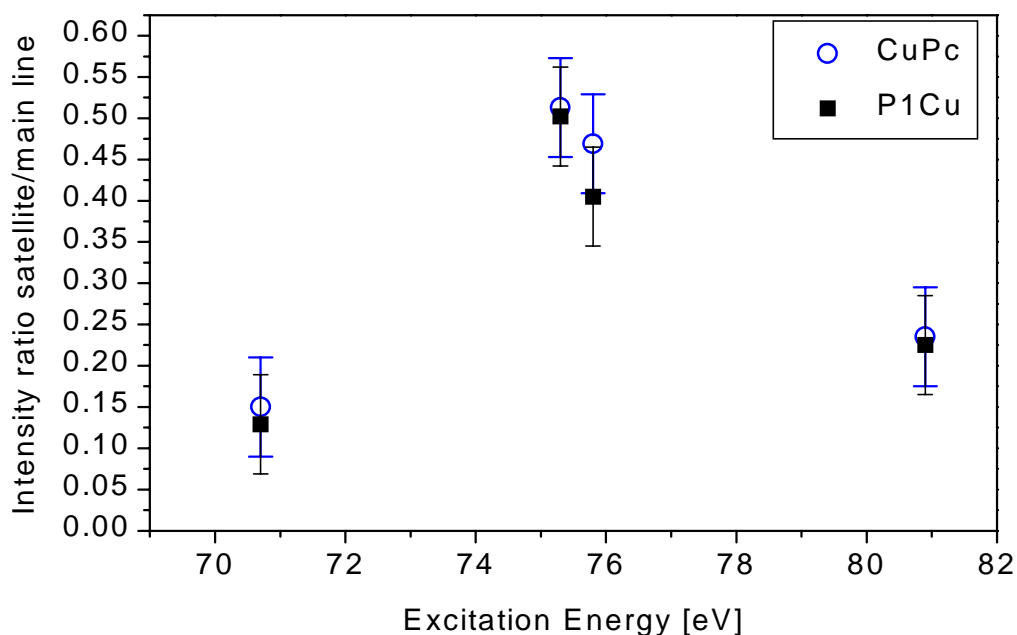

Fig. 5.4-7 Intensity ratio between the satellite at the position of band F' and main line for P1-Cu and CuPc at 70.7, 75.3, 75.8 and 80.9 eV excitation energy. The thicker lines with larger cap widths represent the error bars for CuPc while the thinner lines with shorter cap widths symbolize the error bars for P1-Cu.

Fig. 5.4-7 presents the determined values for the ratio between satellite and main line for unsubstituted CuPc and P1-Cu at two off-resonant excitation energies, (70.7 and 80.9 eV), and at two energies for which the resonant effect is close to the maximum (75.3 and 75.8 eV). For obtaining this figure only the satellite contributions found at the position

of band F', which are the major part of the satellite photoemission features, were taken into account. By considering the range of the error bars, one concludes that P1-Cu and CuPc have similar values for the intensity ratio between satellite and main line, so the tert-butyl substitution does not affect this value.

The intensity ratios between satellite and main line for P0-Cu, P1-Cu, and P2-Cu at the two off-resonant excitation energies (70.7 and 80.9 eV) and at the resonant excitation energies (75.3 and 75.8 eV) are presented in Fig. 5.4-8. The upper panel displays the results obtained by integrating the signal of the satellite peaks at the position of band F' and the lower one accounts for the extended satellite features range, i.e. integration at the positions of bands F and F'.
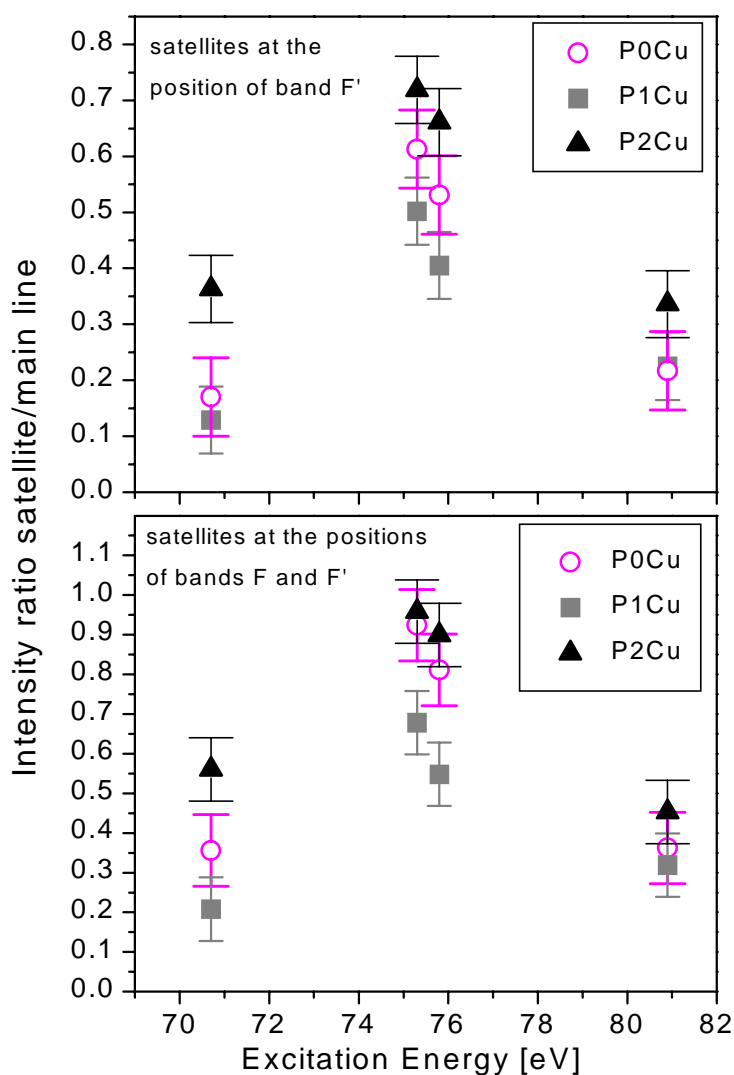

Fig. 5.4-8 The intensity ratio between the satellite and main line for P0-Cu, P1-Cu, and P2-Cu at 70.7, 75.3, 75.8 and 80.9 eV excitation energy.

Thus, the characterization of the copper compounds from the point of view of intensity ratio between the satellite in the valence region and the Cu3d main line has been performed for conditions of maximum and minimum effect, i.e. on and off-resonance. These data represent average values determined after analysis of several data sets for each compound. The error bars for the ratio values in the case of P0-Cu compound are larger than for the other two. This is due to the previously mentioned aspect that for this compound the copper contributions are more difficult to determine.

According to Kawai et al. [KTI94], the charge transfer from the ligand into the copper orbital is larger for covalent cupric compounds than for ionic ones. As a consequence, the ratio between satellite and main line in the core levels region can be regarded as a measure of the covalency, or a measure of the mixing of a covalent state with an ionic state (the ratio is small for covalent compounds and large for ionic ones) [KTI94]. Similar arguments should also hold for the valence region. In case of phthalocyanines it was established that the bonding between the central metal and ligand is not purely ionic, but significantly covalent [LiS2001].

For P0-Cu, P1-Cu and P2-Cu no shoulders are observed at the Cu2p main lines, in addition, the latter have close binding energy values. This indicates that all copper ions in the corresponding films have formally a $3d^9$ initial configuration. Based on the Ref. [KTI94], the increase of the ratio between the $Cu2p_{1/2}$ satellite and main line with the extension of the ligand signifies that the ionic character of the bond between Cu and porphyrazine ligand increases with the size of the molecule. This implies that the delocalization of the Cu3d electrons decreases upon the addition of benzo-units (increasing of the π-electron system of the ligand).

Concerning the valence region, within the error bars range, it can be appreciated that the values of the intensity ratio between satellite and main line at the two off-resonant energies (70.7 and 80.9 eV) support the above-mentioned conclusion from the XPS measurements. This seems true even if the satellite/Cu3d main line intensity ratio for P0-Cu appears in certain cases slightly larger than for P1-Cu. In this light, for resonant excitations one would expect the strongest resonant enhancement of the satellite peaks for the compound with the smallest delocalization of the $Cu\,d_{x^2-y^2}$ orbital, that is the complex with the largest ionic component in the bond between the central copper and ligand. Therefore the strongest resonant enhancement is expected to be observed for P2-Cu. In order to verify that, we have calculated the difference between the satellite/main line intensity ratios at resonant and off-resonant excitations. In the calculations were considered

the satellites at the position of band F'. The results are illustrated in Fig. 5.4-9. The absolute resonant enhancement for P2-Cu appears generally larger than for P1-Cu, as expected, but the value for P0-Cu proves to be comparable with that of P2-Cu. The fact that the overall expected trend is not observed, is attributed to the large error bars associated with the values for resonant enhancement. Also, an important factor determining the resonant enhancement of P0-Cu out of the expected trend is the already mentioned fact that the P0-Cu and P0-H_2 spectra could not always be overlapped at all ligand features, which led to larger values of the satellite/main line intensity ratio for P0-Cu.
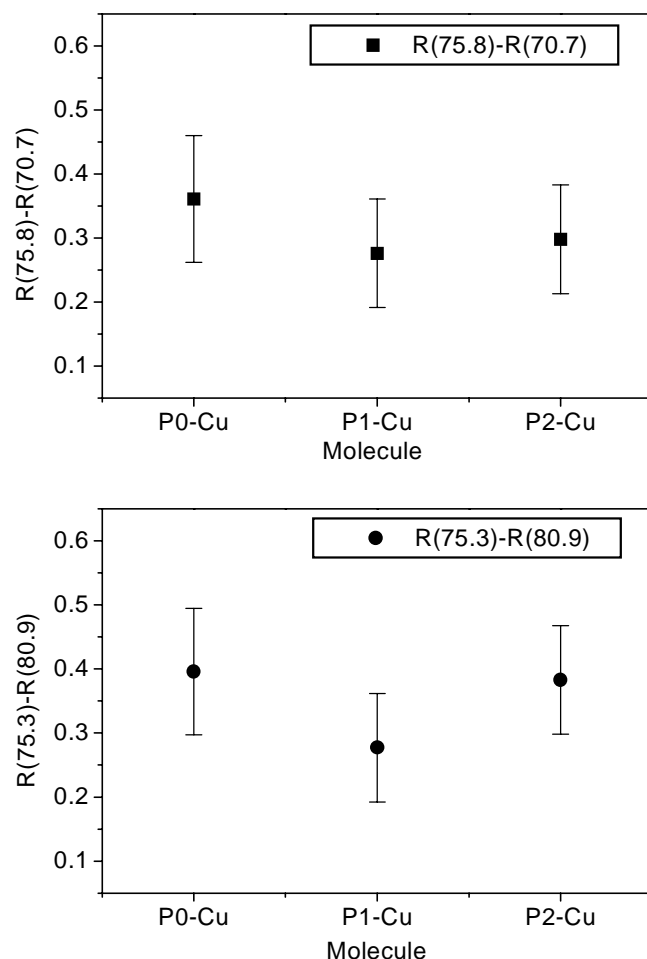

Fig. 5.4-9 The difference between the satellite to main line intensity ratios at resonant and off-resonant excitations (resonant enhancement). In these calculations were considered the satellites at the position of band F'. The values R(75.8)-R(70.7) mean the difference between the satellite to main line intensity ratio for 75.8 eV photon energy and the satellite to main line intensity ratio for 70.7 eV. R(75.3) and R(80.9) represent the satellite to main line intensity ratio for 75.3 and 80.9 eV photon energy, respectively.

Thus, by analyzing the satellite/main line intensity ratios at on-resonant excitations is concluded that within the limits of the present error bars no clear trend can be observed for the satellite resonant enhancement in the spectra of P0-Cu, P1-Cu, and P2-Cu.

We consider that an increased ionic character of the bond between Cu and ligand as result of linear benzoannelation can be correlated with the dimension of the central molecular ring. Orti et al. [OCP96] calculated that for unsubstituted metal-free compounds the size of the C_8N_8 central ring increases slightly but continuously with linear benzoannelation, the distance between the opposite pyrrole nitrogen atoms becoming larger. Considering the similarity between the set of P0-Cu, P1-Cu, P2-Cu compounds and the set of molecules used for those calculations, it seems reasonable that this effect is present in the current series of porphyrazines as well. Thus, the variation in the C_8N_8 inner ring size is a plausible explanation for the variation of the satellite/main line intensity ratio observed for the different copper compounds in identical measurement conditions. The increase of the central C_8N_8 ring size at the extension of the ligand determines a smaller overlap between the orbitals of copper and nitrogen as the distance between the opposite pyrrole nitrogen atoms lengthens. As a direct result, the ligand-to-metal (nitrogen to copper) charge transfer reduces with increase of the ligand size.

5.5 Summary

In this chapter UPS, XPS and NEXAFS measurements on copper porphyrazines were discussed. In particular, the evolution of the valence region and the decrease in the HOMO-1 binding energy with stepwise linear benzoannelation were studied. Near 75 eV excitation energy an enhancement of the copper satellite found in the valence region occurs for P0-Cu, P1-Cu and P2-Cu but not for P3-Cu. XPS and NEXAFS measurements proved that in the P3-Cu film the central copper in the molecules has a $3d^{10}$ configuration (which explains the absence of the resonant effect), while in case of P0-Cu, P1-Cu and P2-Cu the central copper has a $3d^9$ configuration. It is not clear at this point if the $3d^{10}$ initial configuration of Cu in P3-Cu is an intrinsic property of the material or a consequence of the preparation method used for this film. The intensity ratio between the $Cu2p_{1/2}$ satellite and the $Cu2p_{1/2}$ main line increases with the ligand size for the first three complexes in the series. Within the limits of error, in the valence region a similar dependence is evidenced for the ratios between the intensities of the satellite and main line at off-resonant excitations but no clear trend could be identified for the resonant enhancement of the

satellite peaks. Thus, is concluded that the ligand-to-metal charge transfer reduces with increasing ligand size. Based on the Ref. [KTI94], the increase of the satellite/main line intensity ratio with molecular size is interpreted as a result of the increase in the ionic character of the bond between the central copper and the ligand, due to the expansion of the central C_8N_8 porphyrazine ring (increase of the distance between the opposite pyrrole nitrogen atoms).